# FABRICATION OF SUPERHYDROPHOBIC STAINLESS STEEL MESH FOR EFFICIENT OIL WATER SEPARATION

by

Shubham Kumar

A Research Study Submitted in Partial Fulfillment of the Requirements for the Degree of Master of Engineering in Nanotechnology

Examination Committee: Dr. Tanujjal Bora (Chairperson)
Dr. Loc Thai Nguyen
Dr. Bhawat Traipattanakul

Nationality: Indian
Previous Degree: Bachelor of Technology in Electrical and Electronics Engineering
Jawaharlal Nehru Technological University,
Hyderabad, Telangana, India

Scholarship Donor: AIT Fellowship

Asian Institute of Technology
School of Engineering and Technology
Thailand
December 2021

# AUTHOR'S DECLARATION

I, Shubham Kumar, declare that the research work carried out for this research project was in accordance with the regulations of the Asian Institute of Technology. The work presented in it are my own and has been generated by me as the result of my own original research, and if external sources were used, such sources have been cited. It is original and has not been submitted to any other institution to obtain another degree or qualification. This is a true copy of the thesis, including final revisions.

Date: November 18, 2021

Name (in printed letters): SHUBHAM KUMAR

Signature:

# ACKNOWLEDGMENTS

Firstly, I would like to thank my advisor Dr. Tanujjal Bora for his continuous guidance, support and encouragement during this research study. His immense knowledge helped me a lot in progressing my research. I deeply appreciate the time and effort he put on me.

I would also like to thank my committee members Dr. Loc Thai Nguyen and Dr. Bhawat Traipattanakul for their valuable comments and suggestions which helped me improve my research work.

I extend my gratitude further to the Asian Institute of Technology (AIT) for providing me the AIT fellowship during my master's degree here at AIT.

Finally, I express my gratitude to my parents and friends for their continuous encouragement and unfailing support throughout the course and through the process of writing research.

# ABSTRACT

Separation of oil or oily contaminants from water, introduced primarily by various industrial and household applications, is becoming crucial these days to ensure a clean and safe environment. In this study we fabricate a superhydrophobic stainless steel mesh by a one-step electrodeposition technique. The superhydrophobic coating is composed of cerium oxide ($CeO_2$) nanostructures modified with meristic acid, which was characterized by using field-emission scanning electron microscope (FE-SEM) to investigate the morphology of the coating. The water and oil contact angles were measured using an optical contact angle interface tensiometer. Under the optimum conditions, the water contact angle on the coated stainless steel mesh reached up to 150.1 ± 2º which showed superhydrophobcity with sliding angle of 12.6º. The superhydrophobic coated stainless steel mesh showed excellent oil separation efficiency of 98.7% from a mixture of oil in water.

**Keywords: Superhydrophobic, Field-Emission Scanning Electron Microscope, Morphology, Contact Angles**

# CONTENTS

# LIST OF FIGURES

**Figures** **Page**

# LIST OF TABLES

# CHAPTER 1
# INTRODUCTION

## 1.1 Background of the Study

Oil-water separation is considered as a major global issue which needs to be resolved effectively because it contaminates the fresh and sea water which eventually affects the marine life. There are many methods in practice right now for the removal of oil contaminants in water, but not effective (Gupta et al., 2017). Economically it can be very expensive as well to separate oily waste from water, especially when a large amount of oil contaminants are present.

Recent advancement in technology has introduced many new techniques such as polymer dominated filtration membrane, ceramic filtration membrane, nanomaterial based membrane, sponge based filter etc. Polymer based filtration membrane involves polymers like polysulfone and polyvinylidene fluoride (PVDF) which is used for the treatment of oil-water mixture. But due to the intrinsic property of polymers it provides many limitations which can be improved by many techniques such as blending and surface modification. Blending is a process which is used to modify or change porous filtration membrane and it has three main components hydrophilic polymers, amphiphilic copolymers and inorganic nanoparticles.(Zhu et al., 2014)

Amphiphilic copolymers which contains both hydrophilic as well as hydrophobic segments is talked about now a days. The hydrophilic segments helps in enhancing the membrane hydrophilicity and the hydrophobic segment helps in enhancing compatibility with host polymers. Surface modification is another techniques by which we can improve the surface contamination. It involves the chemical reaction by depositing hydrophilic or hydrophobic layer.

Ceramic based membrane is a membrane which has very good thermal, chemical and mechanical stability and it enables their use in severe conditions such as corrosion and high temperature condition. Another recent technologies includes nano-materials based

advanced membrane. For an ideal membrane it is supposed to have thin separation layer and effective pore size. Recently there is one ultrathin filtration membranes was developed using nanomaterial and advanced technologies. They made ultrathin free-standing single-walled carbon nanotube (SWCNT) which has effective pore size is from 20 – 200 nm with very high separation efficiency.(Zhu et al., 2014) There is also a recent paper which suggests the conversion of stainless steel mesh to a hydrophobic mesh by depositing silica particles. This method uses dip-coating to make the surface hydrophobic or superoleophilic. The contact angle achieved by this method is around 135º which is also less as far as superhydrophoicity is concerned.(B. Li et al., 2015)

Oil-water mixture separation techniques depends on the surface wettability of the filters which includes meshes, films, membranes and absorption materials like textiles, foams, sponges. The super wetting materials which were explained above shows better execution in selectivity and efficiency in oil-water separation, there are still some challenges and technical issues which needs to be solved. There are some advantages of Textiles and fabrics over other filters as they are eco-friendly and biodegradable because of which, these kind of materials are considered to be better substrates for oil-water separation. Due to lots of restriction in recyclability because of water absorption plenty of drawbacks like low absorption rate, small absorption capacity and restricted recyclability are seen. Stainless steel mesh substrate has an advantage over other materials used for oil-water mixture separation (Rao & Engineering, n.d.2019).

### 1.2 Statement of the Problem

Oil-water separation is considered to be a major problem for many industries as it is relatively expensive and if left without separation, it severely affects the environment. The increase within the household and industrial activities have led to oily waste water releasing to our environment which is amongst the major pollutants of the sea and other aquatic ecosystems. It is becoming a threat to the lifetime of the marine animals and have great influence in imbalance of the ecosystem(Rao & Engineering, n.d.,2019).

There are many methods in place to separate oil from oil-water mixture but it is expensive or lack the efficiency. Methods like biodegradation, air flotation using electrochemistry, absorption separation biochemistry techniques are effective but have higher cost and have many limitations in their practical implementations. Lack of selectivity is another issue in several techniques used to separate oil from oil-water mixture.

There are many recent filtration techniques like using super polymer with pH triggered system, hygro/solvent triggered system, ions and chemical triggered system and thermo triggered system.

The issues with the current filter is that since surface wettability is complex scientific problem many traditional methods need to be reconsidered, Second is how can we avoid responsiveness deterioration at the time of separation and the loss of separation ability, Third is oily waste water also contains some heavy metal ions or microorganisms which is not easily separable, Fourth is separation speed, which is also considered to be a major issues for the filters and last but not least is mass production of these filters.(J. J. Li et al., 2018)

Therefore a simple filtration system for separating oil from oil-water mixture which can be cost effective, highly efficient and can be easy to implement is a need of the time. The proposed research addresses this issue and attempts were made to provide a simple one step electrodeposition process to fabricate oil-loving superhydrophobic stainless steel mesh filter for cost effective and efficient separation of oil from oil-water mixture.

### 1.3 Research Questions

2 How can we fabricate or design a filter which is very easy to make and is cheaper than other filters designed before?

3 How can we make a filter which has better efficiency than other filters introduced before?

## 1.4 Objective of the Study

The objective of the study is to fabricate a superhydrophobic stainless steel mesh surface for effective separation of oil from oil-water mixture.

Specific objectives of the research are listed below:-

1. To convert a stainless steel mesh surface to a superhydrophobic surface by using one-step electrodeposition of cerium myristate [$Ce(CH_3(CH_2)_{12}COO)_3$] coating.
2. To construct a filtration system using the superhydrophobic stainless steel mesh and investigate the performance of the filtration system against separation of cooking oil from a synthetic oil-water mixture.

## 1.5 Scope of Study

The scope of study is to implement inexpensive and simple way of oil and water separation by developing superhydrophobic and oleophilic stainless steel mesh by changing wetting properties with the help of electrodeposition process. The study examines the strength of this coating to resist water by evaluating water contact angle on the coating. This study also examines the prospect of using electrodeposition technique as an economic approach for the superhydrophobic coating over the stainless steel mesh. The study will use cerium myristate complex to prepare the superhydrophobic coating.

## 1.6 Organization of Study

In chapter 1, we will talk about the background of the study. What is the problem that we are trying to solve? Ways to overcome the problem, what is the question that this paper raises and solves and the objective of the study. In chapter 2, we will talk about the literature related to the topic of this paper. The literature about the methods we are using and different methods used. In chapter 3, we will talk about the methodologies in brief. In chapter 4, we will explain all the results that we got after we finished our experiment and finally in chapter 5, we will conclude our paper.

# CHAPTER 2
# LITERATURE REVIEW

## 2.1 Theory of Surface Wettability

Wetting is the tendency of liquids to keep the solid surfaces in contact. The intermolecular interactions works between the two media (liquid and solid), which results in wetting. "Wettability studies typically involves contact angle (CA) measurements, which shows the degree of wetting when a solid and liquid interact". A "low CA (< 90 °) means high wettability, and the fluid can disperse over a wide surface area". A "high CA (> 90 °) means low wettability, and the fluid should reduce surface contact and form a compact droplet". When the "CA>150° it indicates that there is minimal contact between the liquid droplet and the surface and corresponds to a superhydrophobic behavior".(Duta et al., 2015)

**Figure 2.1**

*Wetting Behavior of Solid Surface*

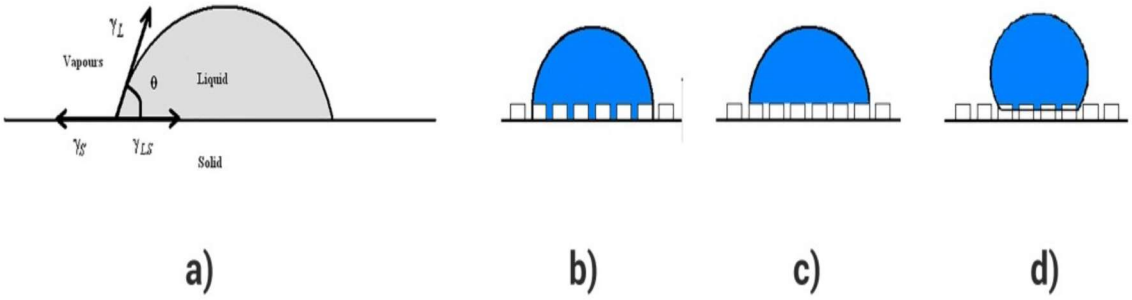


*Note.* Wetting behavior of solid substrates: (a) Young, (b) Wenzel, (c) Cassie, and (d) intermediate state between Wenzel and Cassie regimes.

"The intrinsic contact angle (ICA) of the liquid on the solid surface can be measured using Young 's model if a liquid droplet is relaxed on an ideal smooth solid surface in air (Figure 2.1a)". (Chen et al., 2019)

$$\cos\theta = \frac{\gamma_{SV} - \gamma_{SL}}{\gamma_{LV}} \qquad (1)$$

where "θ" is the ICA of the solid surface with a liquid droplet, the surface tension of the liquid is denoted by $\gamma_{LV}$ , $\gamma_{SV}$ is the surface energy of the solid, and $\gamma_{SL}$ is the interface energy between the solid and liquid". In addition, there are two components of surface energy or tension which is dispersive and non-dispersive. Therefore, total interfacial energy can be written on the solid−liquid interface as,

$$\gamma_{SL} = \gamma_{SV} + \gamma_{LV} - 2\sqrt{\gamma_{SV}^{d}\gamma_{LV}^{d}} - 2\sqrt{\gamma_{SV}^{h}\gamma_{LV}^{h}} \quad (2)$$

where "$\gamma^{d}$" is shown as the surface energy or tension due to the london dispersion force interactions and "$\gamma^{h}$" shows the component of the tension or surface energy because of the dipole−dipole interactions and hydrogen bonding"(Chen et al., 2019). Hence, referring from eq 1 and 2, Young's equation can be expressed as,

$$\cos\theta = \frac{2\sqrt{\gamma_{SV}^{d}\gamma_{LV}^{d}} + 2\sqrt{\gamma_{SV}^{h}\gamma_{LV}^{h}}}{\gamma_{LV}} - 1 \quad (3)$$

Generally, the contact angles (CAs) is much smaller with oil than water for the dispersion-dominated surfaces, since the surface tension is less for oil than water. In the meantime, the "$\gamma^{h}$" of oil may be overlooked as oil is normally nonpolar, so that the ICA of oil ($\theta_O$) and water ($\theta_W$))" may be written as,

$$\cos\theta_o = \frac{2\sqrt{\gamma_{SV}^{d}\gamma_{OV}^{d}}}{\gamma_{OV}} - 1 \quad (4)$$

$$\cos\theta_w = \frac{2\sqrt{\gamma_{SV}^{h}\gamma_{WV}^{d}} + 2\sqrt{\gamma_{SV}^{h}\gamma_{WV}^{h}}}{\gamma_{WV}} - 1 \quad (5)$$

Thus, by changing surface energy of a solid, various surfaces with specific wettability can be fabricated which are hydrophobic / oleophobic, hydrophilic / oleophilic, hydrophilic /

oleophilic, or hydrophobic / oleophilic. Some surface energy values of water (and common hydrocarbon) with dispersion and non-dispersion are listed in Table 2.1. Therefore, the contact angles (CAs) is much smaller with oil than water for the dispersion-dominated surfaces, since the surface tension is less for oil than water.(Chen et al., 2019)

**Table 2.1**

*Surface Free Energy of Various Liquids(Chen et al., 2019)*

| Liquid | Surface Free Energy (mN m-1) | Non Dispersive Component (mN m-1) | Dispersive Component (mN m-1) |
|---|---|---|---|
| Decane | 23.4 | 0 | 23.4 |
| Dodecane | 24.9 | 0 | 24.9 |
| Headecane | 27.1 | 0 | 27.1 |
| Soyabean Oil | 45.5 | 2.5 | 43.0 |
| Water | 72.1 | 50.8 | 21.3 |

However, "Young's equation is only applicable for ideal flat surfaces". Wenzel defined that the "definite surface area of a rough surface is higher than its expected surface area (Figure 2.1b), and proposed a modified model characterizing the influence of roughness on the wettability of rough surface",

$$\cos \theta' = r \cos \theta \qquad (6)$$

where "$\theta'$ is the contact angle of a liquid droplet on a rough surface and r is roughness which is defined as the ratio of the definite surface area to the expected area". It can be seen from the equation that the surface Roughness can improve the solid surface wettability to the extremes of superhydrophilicity or superhydrophobicity (Chen et al., 2019). Especially, when the "air is trapped between the rough structures and droplet spaces and the three-phase, solid / liquid / air interface forms (Figure 2.1c), the CA of a liquid droplet on that surface is given by equation the cassie's equation",

$$\cos\theta'' = f\cos\theta + f - 1 \qquad (7)$$

where “f is the fractional area of the solid−liquid interface underlying the area of contact”.

**Figure 2.2**

*Diverse Superwetting Surfaces*

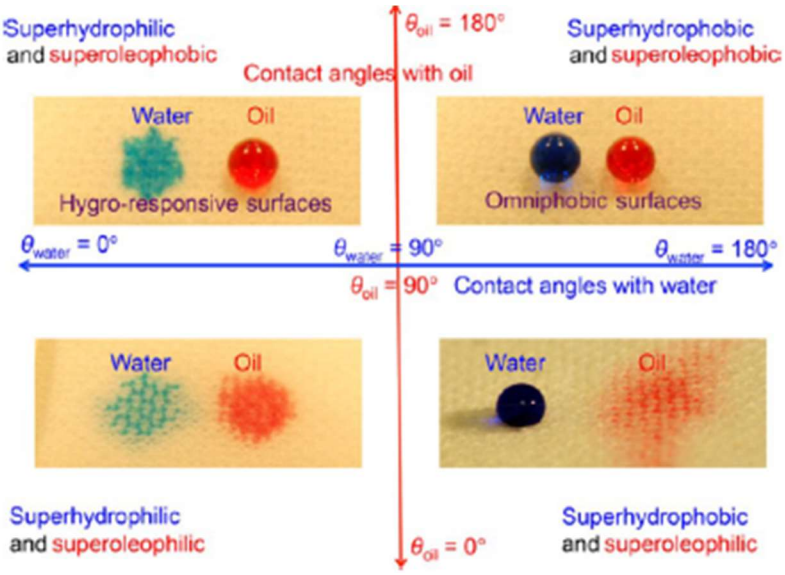


*Note.* superhydrophobic/superoleophobic (top right), superhydrophilic/superoleophobic (top left), superhydrophilic/superoleophilic (bottom left) and superhydrophobic/superoleophilic (bottom right) realized via adjusting the chemical components and surface structures

Thus, multiple superwetting surfaces can be realized by just adjusting the solid surface energy and making dual micro-/nano-surface structures, that are superhydrophobic or superoleophobic,superhydrophilic or superoleophobic, superhydrophilic or superoleophilic, and superhydrophobic or superoleophilic as shown in figure 2.2.(Chen et al., 2019)

## 2.2 Surface Wettability and Oil-Water Separation

Solid surface wettability is an important property because it plays a major role in everyday life and industrial applications. Due to their extensive uses in protective fabrics, self-cleaning surfaces, anti-adhesive and microfluidic devices, the most talked about topic of

interface chemistry in recent years have been surfaces with a water contact angle (CA) greater than 150 ° i.e superhydrophobic surface.(Wang et al., 2011)

A group of researcher from Jiang research group used superhydrophobic/superoleophilic (SHBOI) surfaces for oil-water separation. They used a homogeneous emulsion which has "low-surface-energy material polytetrafluoroethylene (PTFE), the adhesive polyvinyl acetate, the anionic surfactant sodium dodecyl benzene sulfonate", and then water was spray-coated onto stainless-steel-mesh substrates. The substrate was then dried to remove water, sufactact and adhesive and preserving the nano structure of PTFE. Due to the nano / microscale hierarchical roughness combined with the hydrophobic chemical composition of the mesh, the water contact angle $\theta_{CA}$ of this coated mesh is greater than 150 ° and that of diesel oil is about 0 °.

To produce SHBOI mesh with a bead-on-string morphology from thermoplastic polyurethane (TPU), they used electrospinning technology. Firstly, TPU was supended in a mixture of N , N-dimethylformamide and tetrahydrofuran and the TPU solution was then electrospuncted onto a copper-mesh substrate. Then upon treatment with hydrophobic silica nanoparticles, became superhydrophobic/superoleophilic in nature. Due to this special wettability, the coating then stops the water to pass and allows the passage of diesel oil through the mesh. As a result, water and oil mixtures with such SHBOI mesh films may be effectively separated as shown in figure 2.3.(Chu et al., 2015)

A group of researchers prepared a SHBOI copper mesh of polymeric silicone elastomers by aerosol-assisted chemical vapor deposition. The coating of polymer covered all the mesh superhydrohobic with $\theta_{CA}$=152–167°. The water droplets that were dropped and hit the coating surfaca bounced and rolled off while the toluene wetted the surface and passed through the coated mesh quite easily(Chu et al., 2015). The setup is shown in figure 2.3,

**Figure 2.3**

*Examples of SHBOI Copper Meshes for Oil/Water Separation*

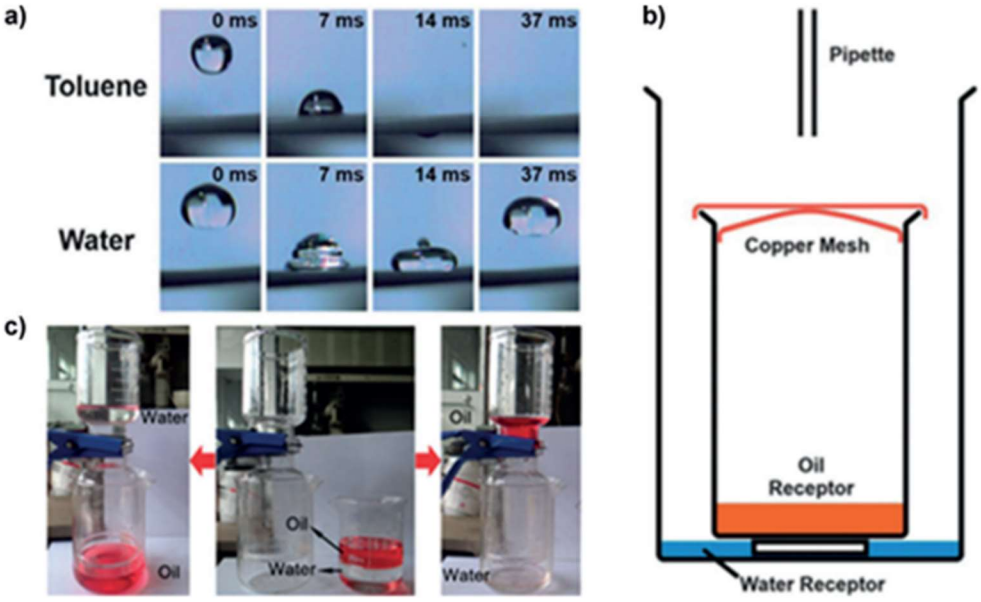


*Note*. a) Photographs showing the interaction of a SHBOI mesh with toluene and water. b) Schematic representation of the separation apparatus developed by Parkin and co-workers. c) Controlled oil/water separation with a pH-switchable surface.

Similarly, a recent paper used superhydrophilic surface for oil-water separation. It prepares a robust superhydrophilic nano-TiO2 decorated on an ultrafiltration membrane made of hierarchical polylactide (PLA) through a spin coating process. The hierarchical PLA membrane surface shows highly hydrophobic surface which has a water contact angle of 107° in 60 s due to the high surface roughness and the underwater superoliophobicity shows oil contact angle of 54° showing certain adhesion to oil underwater. Whereas, $TiO_2$ coated PLA membrane shows a lower adhesion and higher underwater oil contact angle (OCA) of 154±1°, it means that this membrane has very good underwater superoleophobocity.

This happened because the water which was left in the $TiO_2$ coating formed a stable hydration layer to minimize the ability of contact between oil and PLA, thereby providing a possible candidate for oil-water separation.(Xiong et al., 2017)

**Figure 2.4**

*The 3D Images of PLA Membrane*

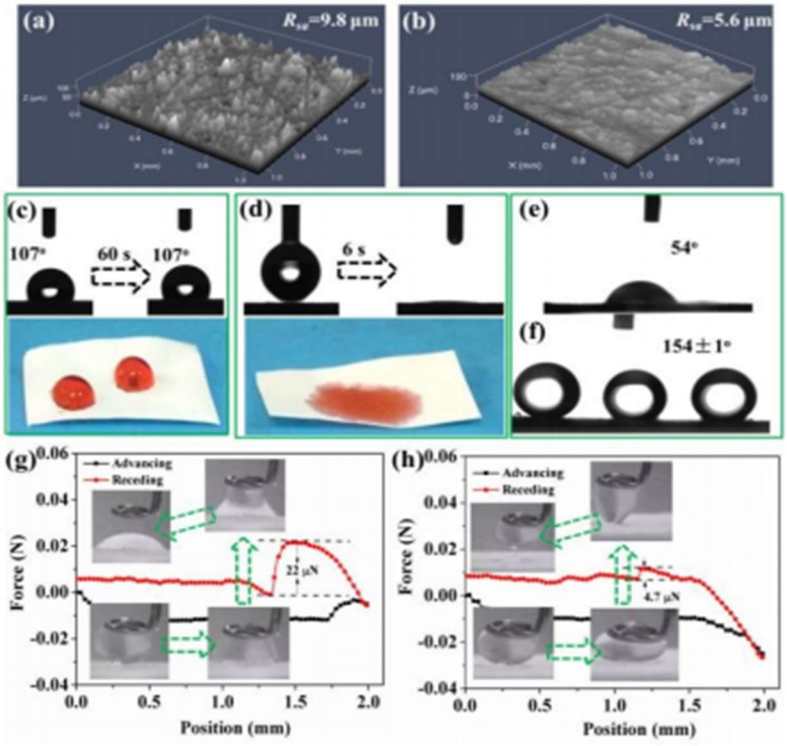


*Note.* (a) the pristine PLA membrane and (b) the TiO2-PLA-1membrane; The water contact angle of (c) the pristine PLA membrane and (d) the TiO2-PLA-1membrane; The oil contact angle of (e) the pristine PLA membrane and (f) the TiO2-PLA1membrane underwater; Real-time recorded force-distance curves for (g) the pristine hierarchical PLA membrane surface and (h) TiO2- PLA-1membrane surface during the dynamic adhesion measurements

## 2.3 Oil-Water Separation using Superhydrophobic Surfaces

There are many methods like gravity separation, adsorption, skimming, solved air flotation, centrifugation, biological treatments and electro coalescence, which were used before for separation of oil-water mixtures but these methods are old, consumes large amount of energy during the separation process, low separation efficiency, easy corrosion and repeated pollution(W. Ma et al., 2018). Therefore there are many new technologies which

has changed the conventional way of separating oil-water separation. Techniques like membrane separation technique(W. Ma et al., 2018), superhydrohobic sponge and cotton for oil water separation (Gao et al., 2018) and electrospinning techniques are currently used for oil-water mixture separation.

In a recent study, we look into a "facile method to fabricate superhydrophobic/superoleophilic membrane by immersing a polyimide (PI)-based nanofibrous membrane". The process of electrospinning was used to prepare PI membranes through imidization by thermally converting PAA nanofibrous membrane. After that, the preparation of the PFDT/PDA/PI membrane was done. (W. Ma et al., 2018)

**Figure 2.5**

*Wettability of the PFDT/PDA/PI Membrane*

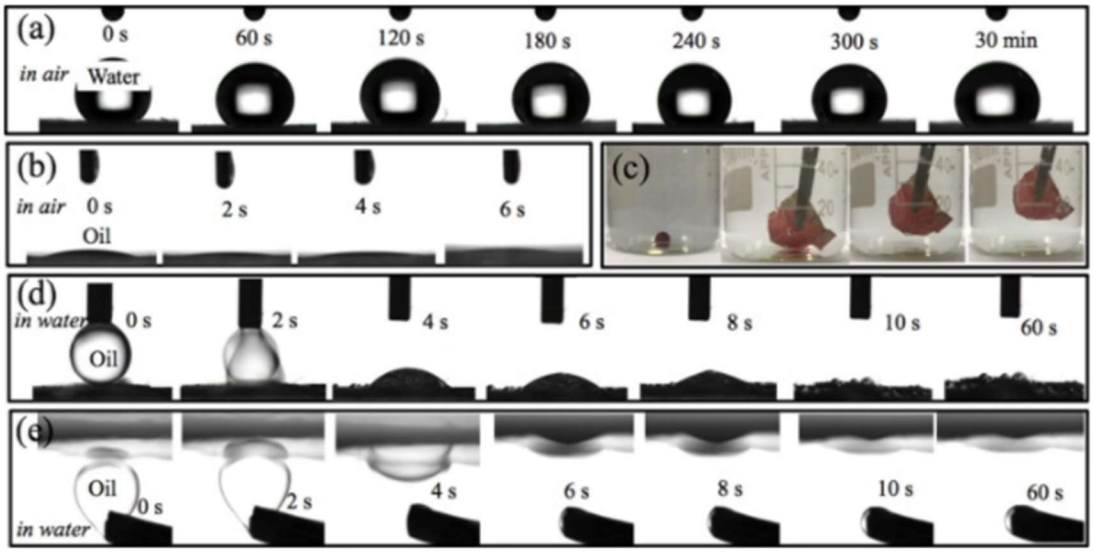


*Note.* (a) Photographs of a water droplet (2 μL) on the PFDT/PDA/PI membrane showing contact angle of 152°; (b) Photographs of an oil droplet (2 μL, n-hexane) on the surface of PFDT/PDA/PI membrane showing nearly zero contact angle in air; (c) Photographs of a DCE droplet (dyed with oil red) in water could be adsorbed by a piece of PFDT/PDA/PI membrane; (d) Photographs of an oil droplet (2 μL, 1,2-dichloroethane (DCE)) on the surface of PFDT/PDA/PI membrane in water; (e) Photographs of an oil droplet (2 μL, n-hexane) on the surface of PFDT/PDA/PI membrane in water

The water contact angle for superhydrophobicity comes around 153 ° and the superhydrophobic performance of the PFDT / PDA / PI membranes continued to be stable for a long time. (W. Ma et al., 2018). The resultant technique as we can say is very efficient, highly flexible and shows high superhydrophobicity for a long time.(W. Ma et al., 2018)

Another technique, which is very simple and uses various substrate for the fabrication of robust superhydrophobic surfaces is phase separation method. This approach uses "polydimethylsiloxane (PDMS) as the binder, tetrahydrofurane (THF) as the solvent, and water as non-solvent". Various kinds of fabrics like cotton (individual diameter 15 μm of cotton fibre), silk, polyester , nylon, acrylic, viscose, ramie, wool and melamine sponge is used for fabrication.(Gao et al., 2018)

**Figure 2.6**

*Different Fabric Superhydrophobicity*

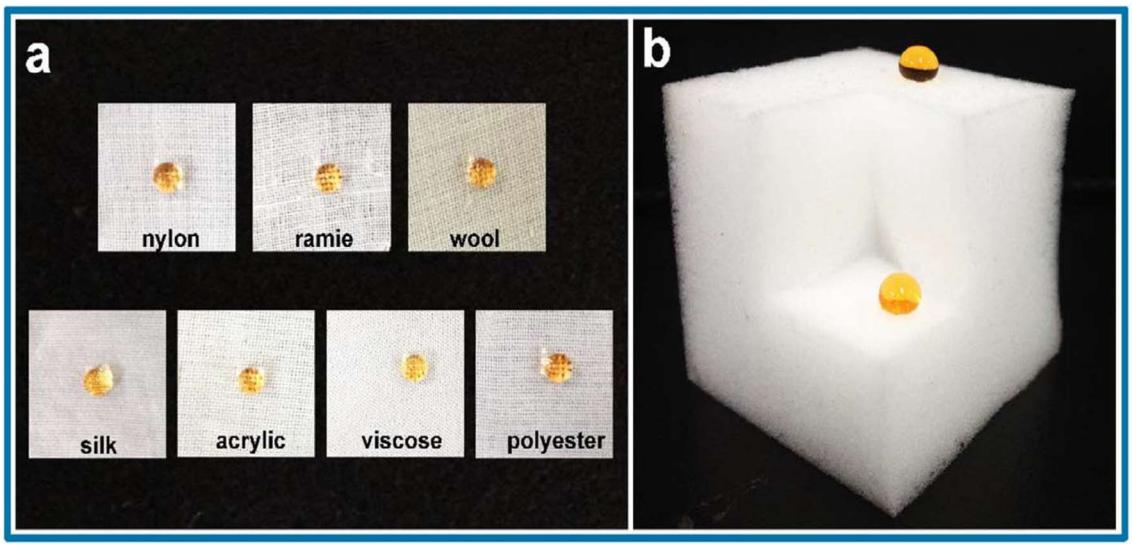


*Note.* Different fabric substrates got superhydrophobic property after modification; (b) commercial sponge obtained superhydrophobic ability on both inside and outside after modification.

It was noteworthy that all substrates exhibited excellent superhydrophobic properties. Furthermore, industrial sponge with melamine was also used as a base. As illustrated in Figure 2.6, the sponge had a uniformly superhydrophobic quality, both indoors and out. Some other strategies such as spraying do not understand this very strong anti-wetting effect.(Gao et al., 2018)

**Figure 2.7**

*Oil-Water Mixture Separation Stages.*

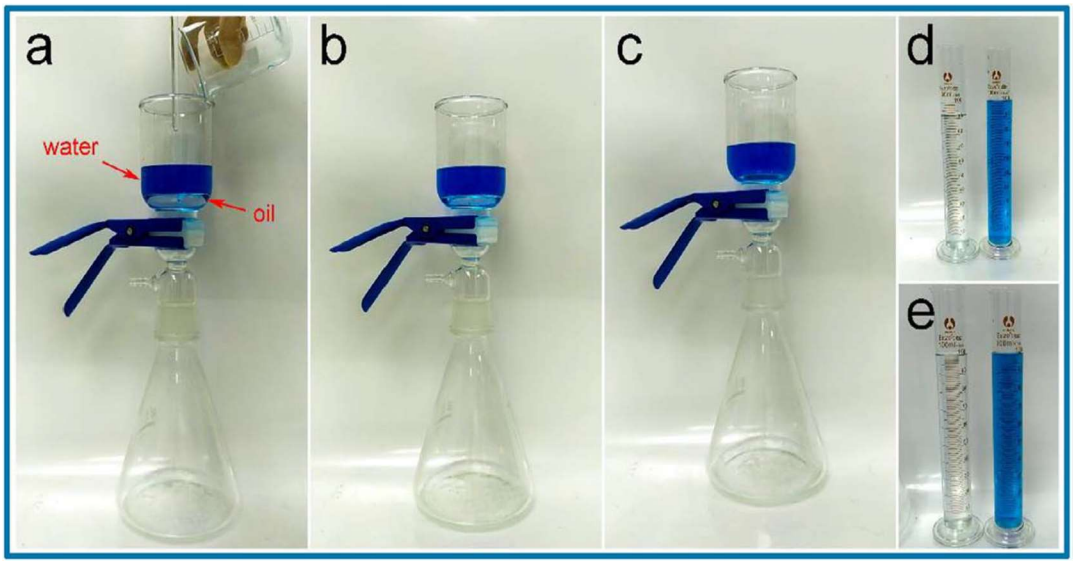


*Note.* Time sequence of the oil-water separation process with modified fabric (a–c); the volume of water and dichloromethane before (d) and after (e) separation.

The as-prepared fabric had an excellent superhydrophobicity with a CA greater than 150 ° and a SA less than 10 °, even if THF to water ratio was 3:7. Moreover, the color of the fabrics hardly changes. By simply altering a 2D fabric and 3D sponge, developed using both surfactant-free and surfactant-stabilized methods, the oil-water mixture can be effectively and easily separated.(Gao et al., 2018)

The above mentioned different techniques have different advantages and dis-advantages, since this technique can be cost effective but the process is pretty complex and we also

don’t know the efficiency of the above technique. The other technique was very efficient and cost effective but the commercial use of that technique was still questionable.

There are still many challenges in the fabrication of superhydrophobic surface or superoliophilic surface but the researcher are trying to make it easy and the one we are preparing is a very simple and cost effective method of fabrication.

### 2.4 Challenges in the Fabrication of Superhydrophobic Surfaces

Production of a superhydrophobic surface is not an issue with modern technologies but maintaining its robustness and surface fragility is difficult under extreme conditions. The robustness of superhydrophobic materials is a key issue for applications such as photovoltaic cells and self-cleaning windows. In these applications the friction and wear tends to weaken and erode the surface over time(M. Ma et al., 2008) . When a superhydrophobic material is exposed to free air for a long time it deteriorates due to the deposition of stains. (Nakajima et al., 2001)

Mechanical durability is another issue when we talk about of superhydrophobic surfaces. Appropriate nano or micro-topographic surface chemistry can achieve a high contact angle and low sliding angle of superhydrophobicity. These kind of structure maybe easy to create using advanced technologies but it is very tough to attain their stability. (Simpson et al., 2015)

Most research has been conducted on flat and hard substrates such as glass slides, metal surfaces and silicon wafers. The majority of the production methods mentioned in the literature are very costly and apply to small flat surfaces or to certain materials. Therefore they are not suitable for large-scale production. (Jeevahan et al., 2018)

For multifunctional applications, other surface functions and superhydrophobicity could be difficult to include for example, high transparency is required on the optical materials. Roughness of the surface scatters more light which diminishes the transparency. (Karunakaran et al., 2011)

The fabrication techniques which are used for superhydrophobic surfaces are top down approach, bottom up approach and Combinational approach. Under “top down fabrication method, the techniques like lithography, templating, micromachining, plasma treatments, etching” etc. are performed and under “bottom up approach techniques like chemical vapor deposition (CVD), and electrochemical deposition, layer-by-layer (LbL) deposition, and sol–gel methods” are performed. In combined approach both the methods are combined with different techniques to fabricate superhydrphobic surface. All these techniques have their challenges which is discussed using a table2.2,(Jeevahan et al., 2018)

**Table 2.2**

*Fabrication Methods for Superhydrophobic Surfaces*

| Fabrication method | Process description | Limitations |
|---|---|---|
| Lithography | “A pattern is transported from master to surface and produces numerous copies, similar to an inked stamp” | The main issue with lithography technique is its increase in cost of fabrication and the size of transistor.(X. M. Li et al., 2007) |
| Template | “Template is a surface that consists of the voids of a given form or pattern. Upon this template a coating material is filled and pressed to form the inverse of the pattern”. | Cost is high and sometimes the patterns are not consistant.(Cao et al., 2007) |
| Electrospinning | “A polymer solution is filled in a capillary tube, and electrically biased. The solution to the polymer is then ejected in jet form”. These fibers are then spun onto the solid surface to create fiber mats (substrate). | To repel oil there is a special kind of polymer is needed i.e fluoropolymer, which has a limitation that it does not hold charge so it doesn’t spin.(Celia et al., 2013) |
| Sol–gel | A chemical precursor is converted into a glassy material while undergoing hydrolysis and polycondensation reactions which forms a layer on the substrate. | A lot of work and time isneeded to optimize the stability of the sol and different type sensor production.(*Disadvantagest Sol Gel Process - Thin Film - Texas Powerful*) |

| Fabrication method | Process description | Limitations |
|---|---|---|
| Layer-by-Layer | "Positive and negative polyelectrolytes are alternatively coated on a surface (substrate) by sequential adsorption by alternatively dipping into the charged solutions". | This process is suitable for covering complex objects, but when it comes to large areas or more numbers of parts it becomes very difficult to utilize this process.(Ariga et al., 2007) |
| Etching | Once an etching medium is applied to a surface, the chemical reactions selectively erode / remove materials. | Disadvantage of the etching techniques is that since the reacting species reacts in many directions generally in plasma etching process, that they don't have high anisotropy and can enter the masking material from underneath.(Shirtcliffe et al., 2011) |
| Chemical vapor deposition | "The phase of a chemical precursor is transformed into a phase of vapor phase and is allowed to react with the heated surface (substrate) to form a thin film layer" | Limitation of CVD is that precursors are mostly hazardous or toxic and the by-products of these precursors may also be toxic.(Cao et al., 2007) |
| Electrochemical processes (oxidation and reduction) | "It is an electrochemical reduction process where metal ions are reduced into metals and deposited". | The use of this technique has been reduced because of high cost of electrodes and concerns about the presence of toxic byproducts in the treated water.(Radjenovic & Sedlak, 2015) |

# CHAPTER 3
# METHODOLOGY

## 3.1 Substrate Preparation

The substrate for this experiment is stainless steel mesh. Firstly, the mesh was cut into (3 x 3) cm after which the cleaning process of stainless steel mesh starts by removing Grease, oil strain and dirt particles. In this experiment we used a stainless steel mesh pores of 200μm diameter and the stainless steel wire of 25μm diameter as a substrate.

Then we placed a beaker in which we put substrate and liquid soap together which was ultrasonicated for 15 minutes with deionised water (DI water). The soap water was removed from beaker and acetone was added then ultrasonicated for 15min. Then again acetone was replaced with DI Water and finally ultrasonicated for 15 min. This process was repeated several times to remove dirt completely and finally the cleaned up samples were kept in petri dish and was kept in oven till the substrate was properly dried.

## 3.2 Electrodeposition of Superhydrophobic Coating on the Stainless Steel Mesh

The electrolytic solution was prepared by dissolving Cerium nitrate hexahydrate (0.05 M) and myristic acid (0.1 M) to methanol. For electrodeposition, power was supplied by direct current (GWINSTEK, GPC-6030D) to stainless steel mesh and graphite plate which was connected together. The superhydrophobic behavior of stainless steel mesh was observed between the range of 10V - 40V. The electrodeposition experiment was conducted at room temperature.

The stainless steel mesh was taken as the cathode and reduction process occurs whereas the graphite plate was taken as the anode, where oxidization occurs. Throughout the experiment the distance between cathode and anode was 2 cm. The specimen was immediately removed and washed with methanol after electrodeposition, and then dried in air.

**Figure 3.1**

*Electrodeposition Process*

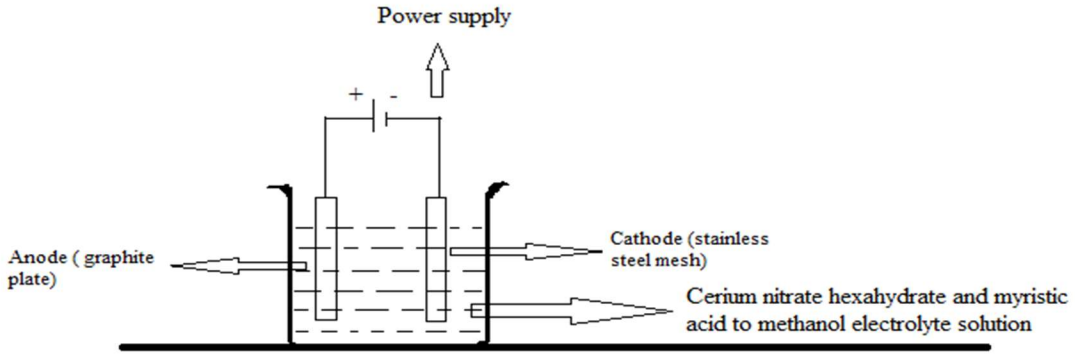


*Note.* Schematic showing electrodeposition process

### 3.3 Characterization of the Superhydrophobic Stainless Steel Mesh

For characterization, we used Field-emission Scanning electron microscope (FE-SEM) for surface morphology of deposited superhydrophobic stainless steel mesh. FE SEM tells us about the roughness of the substrate which tells us about the shape of deposition of nanoparticle.

The measurement of oil and water contact angle was done at three different places which is on left side, middle and right side of the sample and that was investigated for the wetting behavior of the stainless steel mesh. The average of them was taken as the contact angle. Following parameters was evaluated from the measurement: static contact angle (CA), dynamic contact angle, sliding angle and shedding angle.

### 3.4 Oil-Water Separation Apparatus Fabrication

For testing, a separation reactor will be used as shown in figure. The separation reactor was designed by using a software named 123d design. Inside the separation reactor there was a slot made for the stainless steel mesh which was kept in tilted position. The position of separation reactor was decided by the sliding angle. For sliding angle calculation we poured a water droplet on coated/uncoated stainless steel mesh and tilted the substrate and captured the angle at which the droplet slides.

The upper part of setup was kept hollow from where we poured oil water mixture. After it passes the coated stainless steel mesh oil and water was separated. Oil passed through the coated mesh and collected down in the beaker and water slides which was collected in different beaker kept beside it.

**Figure 3.2**

*Experimental Setup*

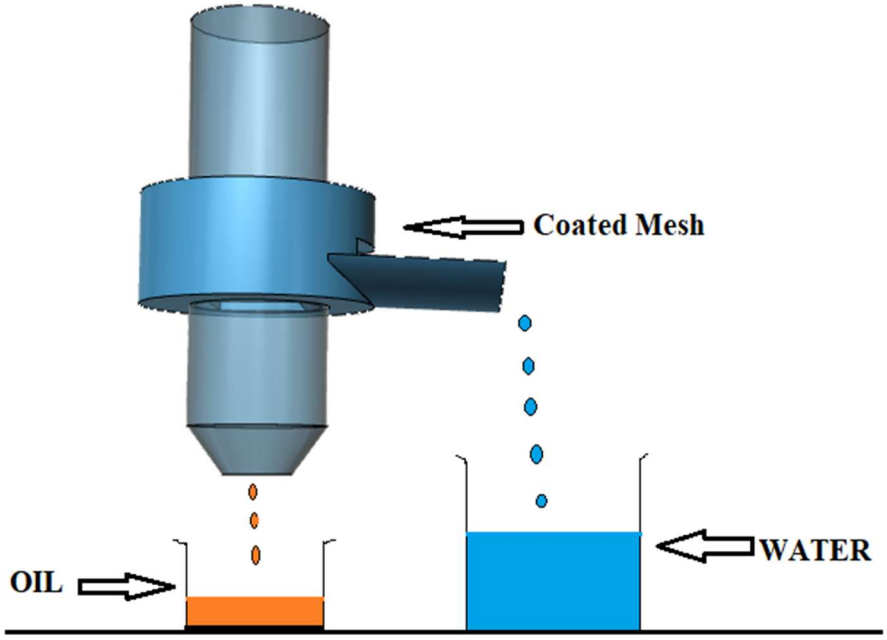


*Note.* Oil water separation experimental setup

### 3.5 Oil-Water Separation Study by the Superhydrophobic Stainless Steel Mesh

The water and oil (sunflower oil) were taken in a beaker with 9:1 volume ratio. The mixture was firstly mixed in a beaker and then stirred for around 10 minutes. Then the oil-water mixture was poured over coated stainless steel mesh and for every separation, a total of 5 mL oil-water mixture was slowly poured and separated by the superhydrophobic stainless steel mesh.

For efficiency test the same procedure was carried out 10 times.

$$\% \text{ efficiency} = \frac{volume\ of\ water\ collected}{volume\ of\ water\ inserted} \times 100 \qquad (8)$$

# CHAPTER 4
# RESULTS AND DISCUSSION

The experiment was performed by dissolving cerium nitrate heahydrate and myristic acid into methanol to make the electrolyte solution. The substrate was taken as stainless steel mesh of size 3 x 3 cm. In the electrodepositon process, graphite plate was taken as anode and stainless steel mesh was taken as cathode. A regulated direct current power source was connected. After the completion of electrodeposition process, stainless steel mesh achieved superhydrophoicity. All the results are explained below.

**Figure 4.1**

*Stainless Steel Mesh*

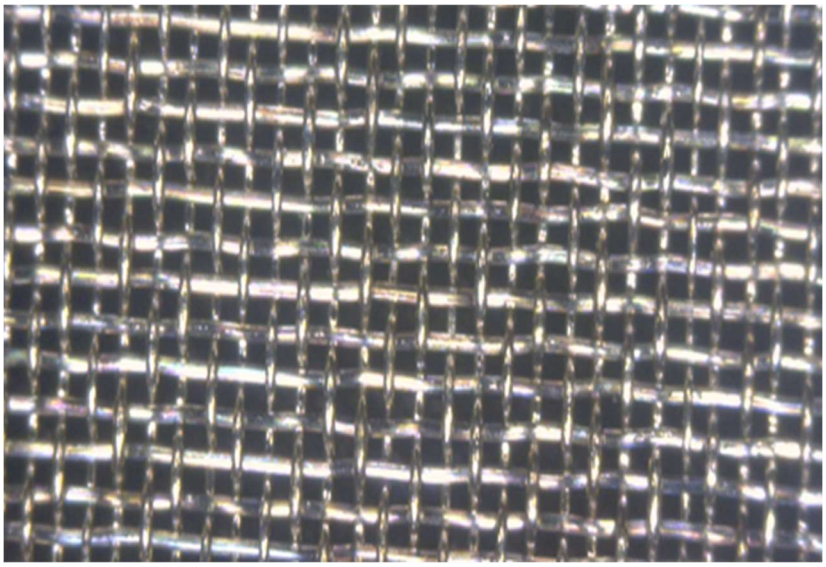

*Note.* Figure of clean and uncoated stainless steel mesh 3x3cm

## 4.1 Surface Morphology

The surface morphology of coated stainless steel mesh is explained by Scanning electron microscope (SEM) images. The Scanning electron microscope (SEM) images were taken at different magnification to better explain deposition and shape of coated nanomaterial

after deposition. All the samples were prepared at a constant electrodeposition time for 10 minutes, and only the voltage were varied.

**Figure 4.2**

*SEM Images of Coated Stainless Steel Mesh with 10V Electrodeposition Voltage*

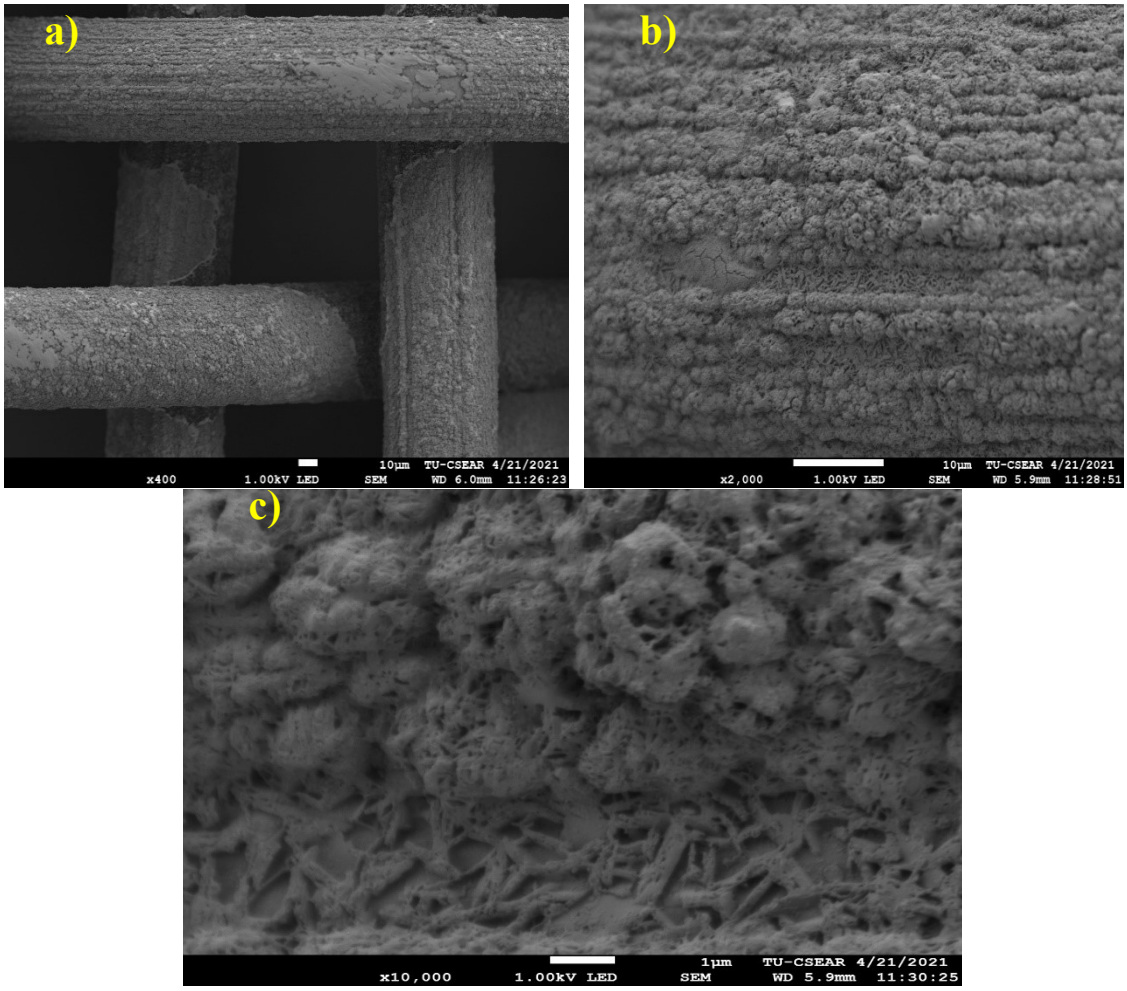


*Note.* (a) 400x magnification (b) 2000x magnification (c) 10,000x magnification

The above figure shows the deposited stainless steel mesh. From the figure 4.2, we can say that cerium myristate is deposited on stainless steel mesh. In this the electrodeposition is done at 10V with deposition time of 10 minutes. Figure 4.2(a) shows the SEM image with 400x magnificaton and we can see mild surface roughness on the substrate. Figure 4.2(b)

shows the more mangnified picture (2000x magnification) of the deposited stainless steel in which cerium myristate nanoparticle has agglomerated.

The cerium myristate which is deposited on the steel wire results in surface roughness and also increases the surface area. The deposition is moderate and no particular flakes were formed in this. The contact angle was observed to be 125.9° $\pm$ 2° which is hydrophobic in nature.

**Figure 4.3**

*SEM Images of Coated Stainless Steel Mesh with 20V Electrodeposition Voltage*

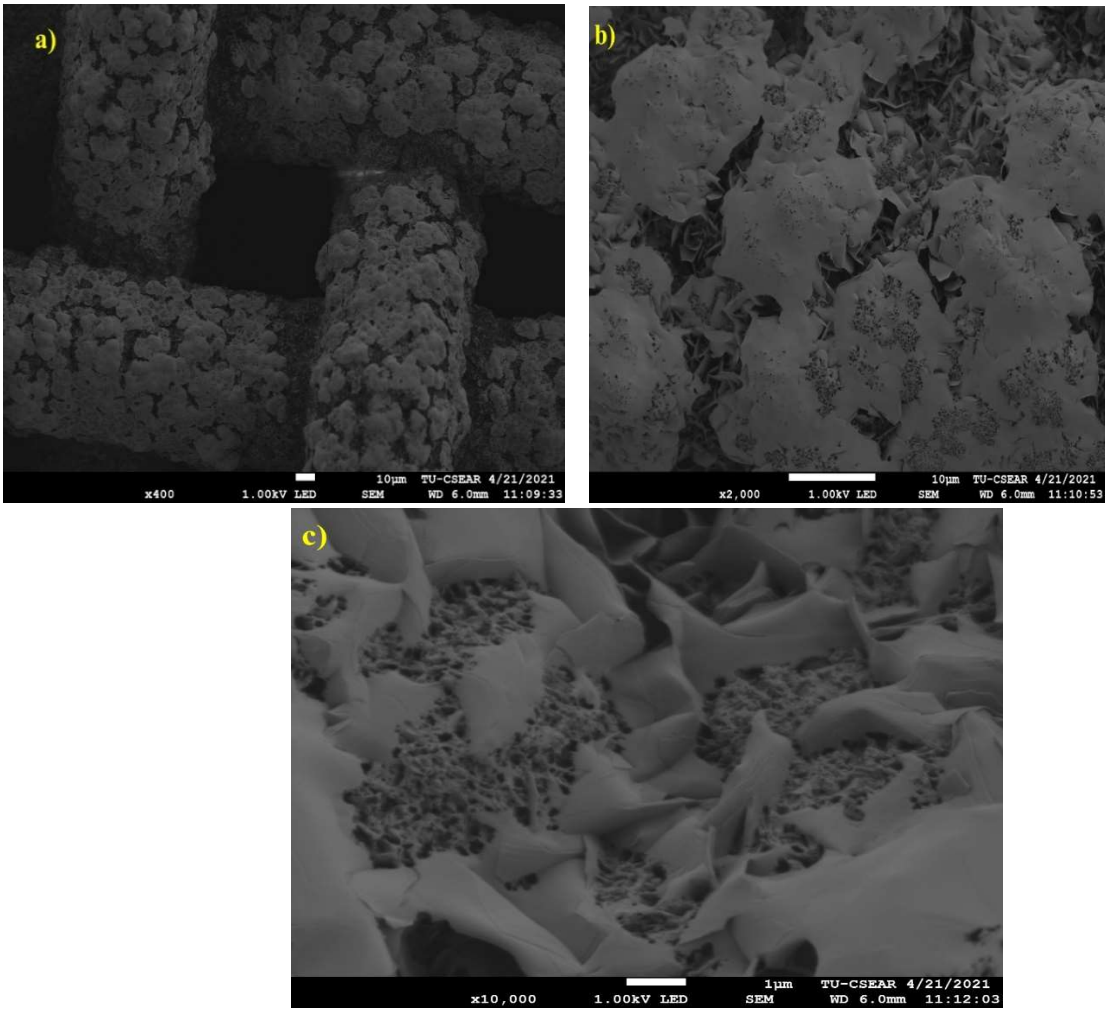


*Note.* (a) 400x magnification (b) 2000x magnification (c) 10,000x magnification

The above figure shows SEM images of stainless steel mesh after electrodeposition at 20V voltage. Comparing the images from Figure 4.2(a), we can observe that the steel wire is fully covered with two layers of cerium myristate in figure 4.3(a), as the layer increased the surface roughness also increases. From the figure 4.3(b) and 4.3(c), as the magnification increases we can clearly observe that the flakes were formed on the upper layer of steel wire and we can say that it has more roughness as compared to the 10V electrodeposited stainless steel wire. The deposition observed here is homogeneous and have uniform distribution.

The space between the deposited cerium myristate nanoparticle and the water droplet also increases because of increased surface roughness. As the surface roughness is more the surface area also more which eventually leads to higher contact angle. The contact angle observed for the substrate with 20V voltage is 150° $\pm$ 2°, which is considered to be superhydrophobic.

**Figure 4.4**

*SEM Images of Coated Stainless Steel Mesh with 30V Electrodeposition Voltage*

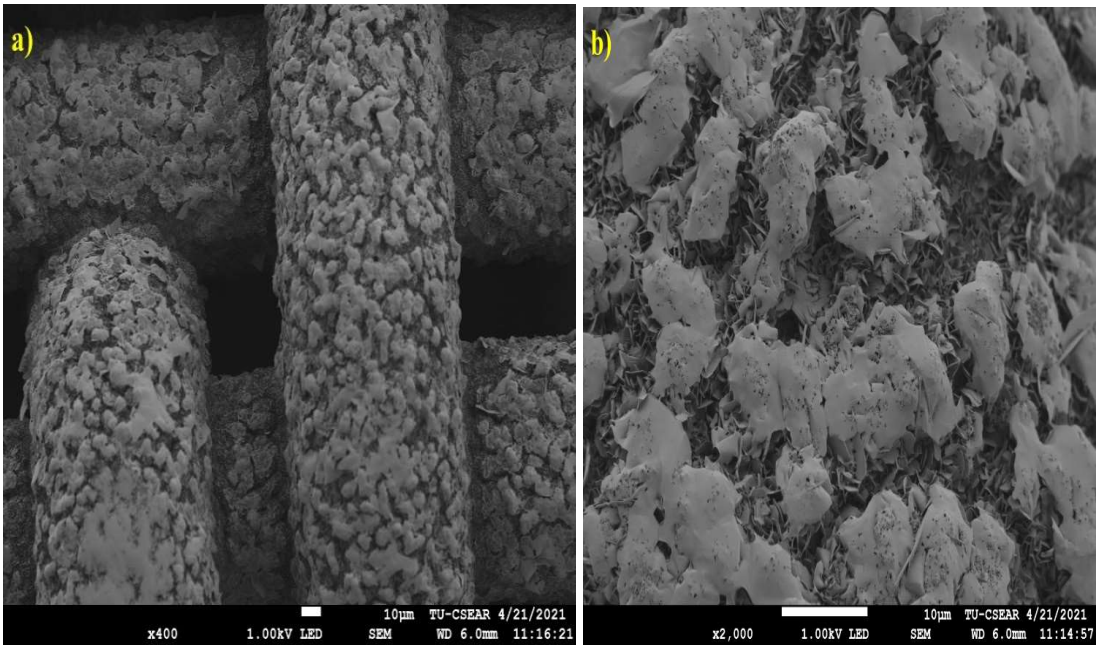

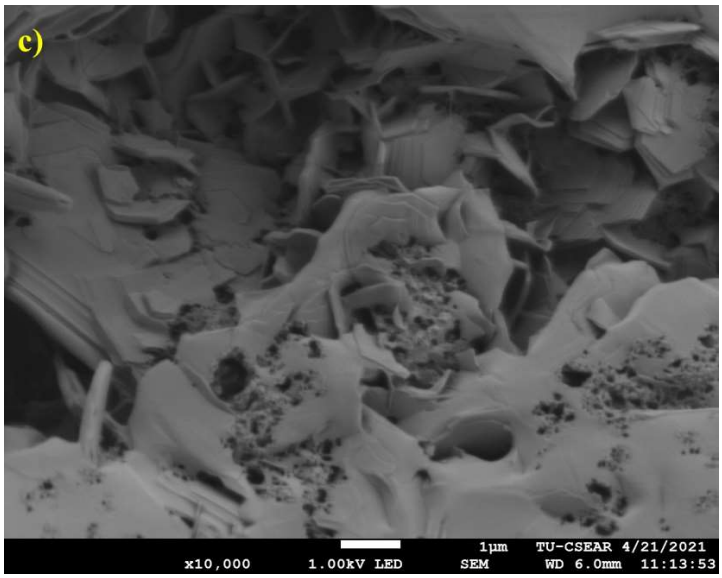


*Note.* (a) 400x magnification (b) 2000x magnification (c) 10,000x magnification

SEM images of electrodeposited stainless steel mesh at 30V voltage at different magnification is shown. From Figure 4.4(a), we can say that the deposition of cerium myristate is quite similar to figure 4.3(a) (400x magnification for 20V steel wire) as same kind of uniform deposition is visible with multiple layer agglomerated but when we see the higher magnificaton from Figure 4.4(b) and 13(c), we can observe that the flakes are formed but are not as consistant or uniform as the 20V electrodeposited stainless steel mesh. The surface roughness here is more as compared to the 10V electodeposited stainless steel mesh.

Since the flakes formed are less as compared to 20V electrodeposited stainless steel mesh, the surface roughness is less which leads to less surface area. The contact angle measured with 30V voltage is $135° \pm 2°$ which is considered to be hydrphobic in nature. From the three different voltages that we have analyzed, 20V electrodeposited stainless steel mesh shows the best result because it has uniform surface roughness and highest contact angle.

**Figure 4.5**

*SEM Images of Coated Stainless Steel Mesh with 40V Electrodeposition Voltage*

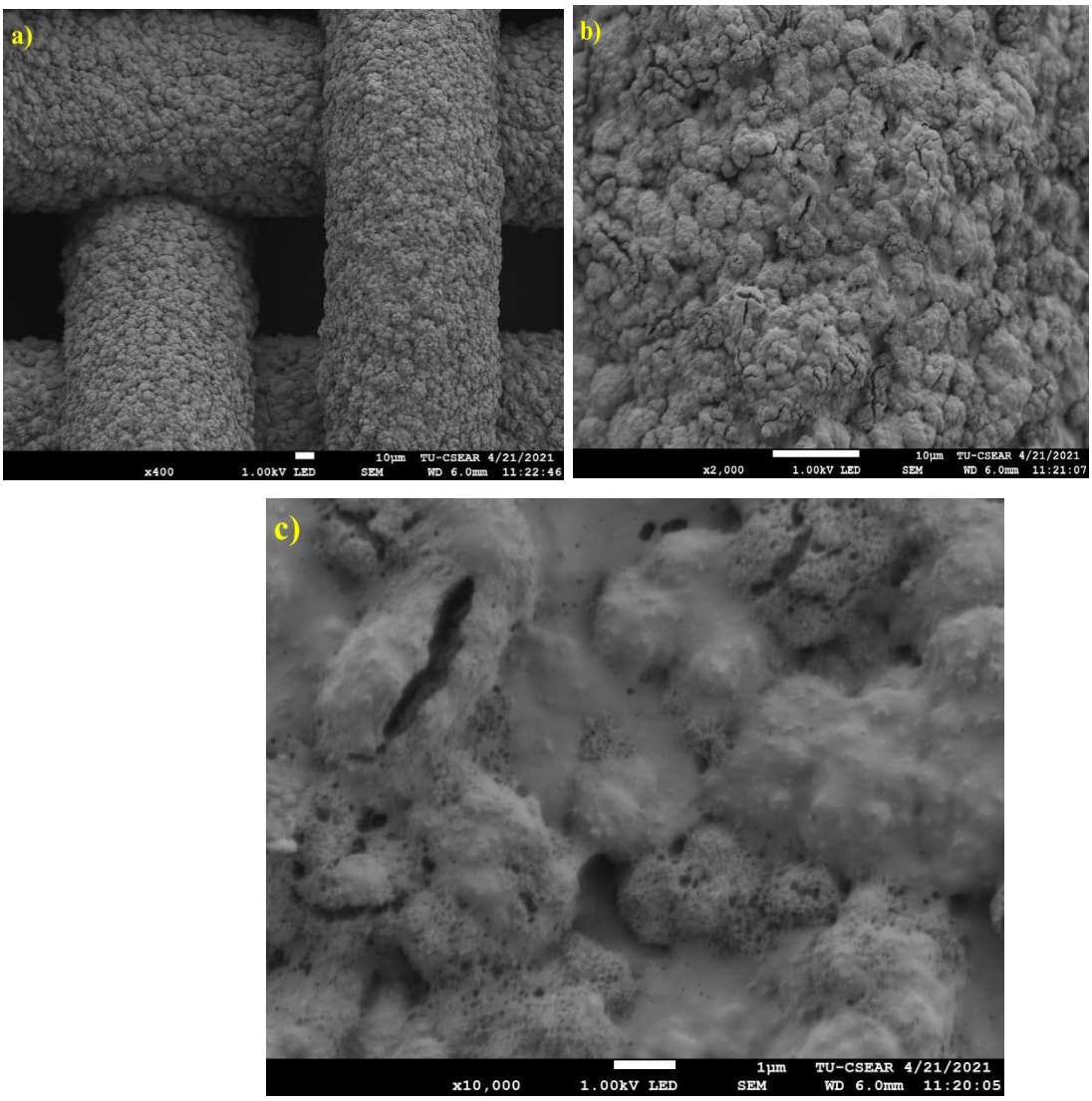


*Note.* (a) 400x magnification (b) 2000x magnification (c) 10,000x magnification

The above figure shows the stainless steel mesh with 40V electrodeposited voltage. From Figure 4.5(a), we can say that the deposition decreased as compared to the 30V electrodeposited stainless steel mesh. The flakes which agglomerated on the surface of steel wire disappeared and it's more of an uneven deposition of cerium myristate nanoparticle. After checking the magnified SEM images from Figure 4.5(b) and 4.5(c), we can clearly say that the surface roughness has decreased and there is no flakes formed.

As the flakes are not formed, the space between the deposited cerium myristate nanoparticles and water droplets is very less as compared to 30V electrodeposited stainless steel mesh. This also decreases the surface area which eventually results in lower contact angle. The contact angle was observed to be $132° \pm 2°$ which is considered to be hydrophobic in nature.

### 4.2 Contact Angles

Wettability is one of the most important behavior of a surface to characterize the different surfaces. Contact angle measurement is a parameter which differentiate the surfaces with different behavior. In this study we have coated the stainless steel mesh with cerium myristate which shows superhydrophobic behavior.

Different electrodeposited voltages influence the surface morphology of coated stainless steel mesh which shows different static contact angle. Starting with 10V electrodeposited voltage, the static contact angle measured is $125.9 \pm 3°$ as shown in the Figure 4.6.

**Figure 4.6**

*Static Contact Angle for Coated Mesh with 10V Electrodeposited Voltage.*

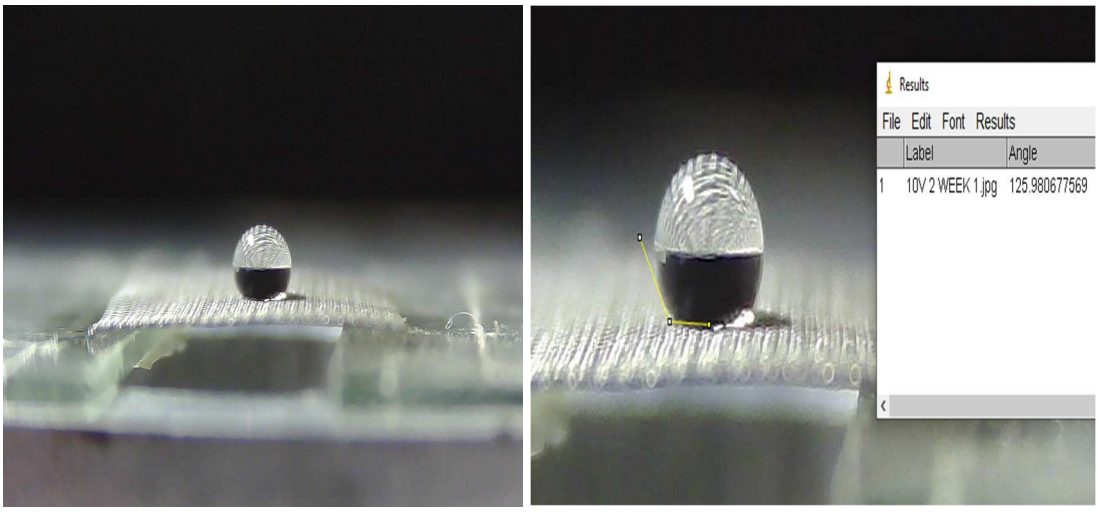


*Note.* Water droplet on 10V electrodeposited stainless steel mesh with static contact angle measurement.

Static contact angle measurement is done by pouring a 10ul drop of water on a coated mesh and left it for some time. After that a software is used named imajeJ to calculate the angle between the water droplet and the surface. For 20V electrodeposited voltage, the static water contact angle was measured to be 150±2° as shown in Figure 4.7.

**Figure 4.7**

*Static Contact Angle for Coated Mesh with 20V Electrodeposited Voltage.*

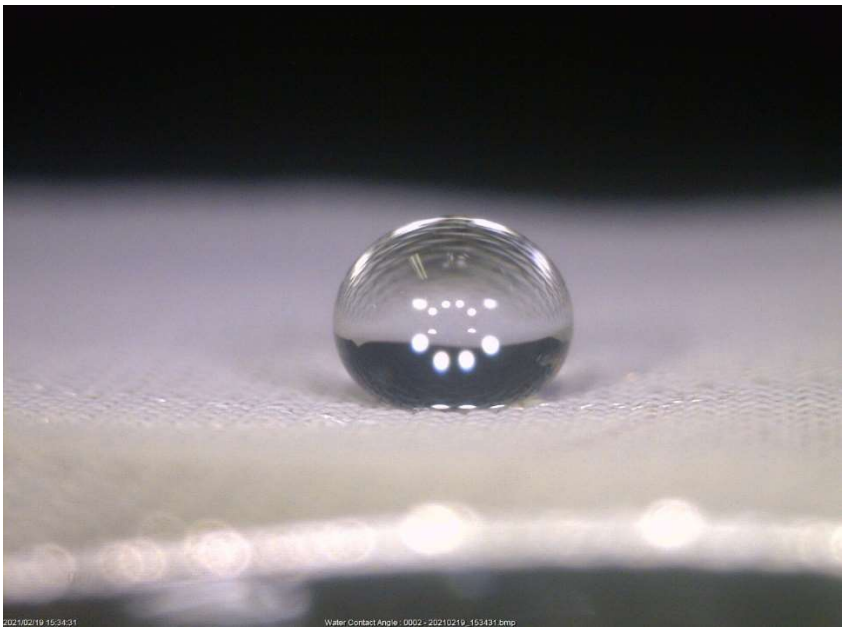

*Note.* Water droplet on 20V electrodeposited stainless steel mesh with static contact angle measurement.

Similarly when the electrodeposited voltage was changed to be 30V, the static water contact angle was measured to be 135±5° as shown in Figure 4.8 and when the same voltage is changed to be 40V, the static water contact angle was measured to be 130±5° as shown in Figure 4.9.

**Figure 4.8**

*Static Contact Angle for Coated Mesh with 30V Electrodeposited Voltage.*

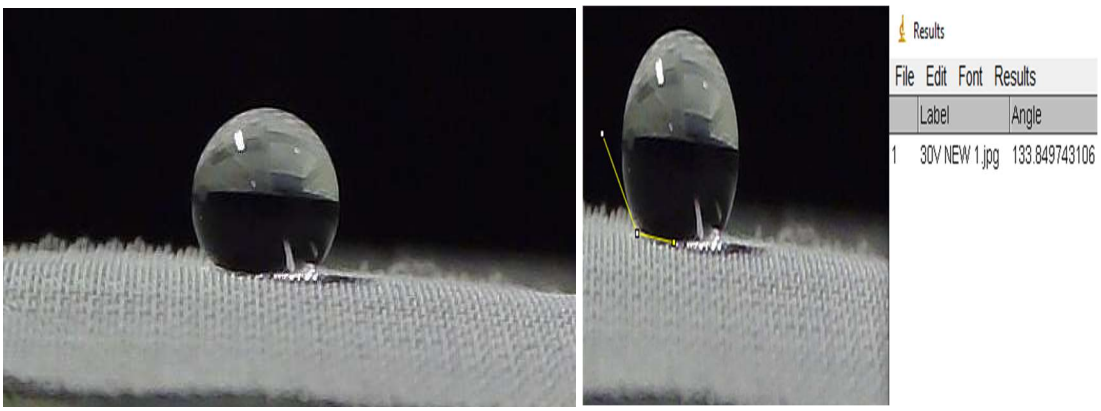


*Note.* Water droplet on 30V electrodeposited stainless steel mesh with static contact angle measurement

**Figure 4.9**

*Static Contact Angle for Coated Mesh with 40V Electrodeposited Voltage.*

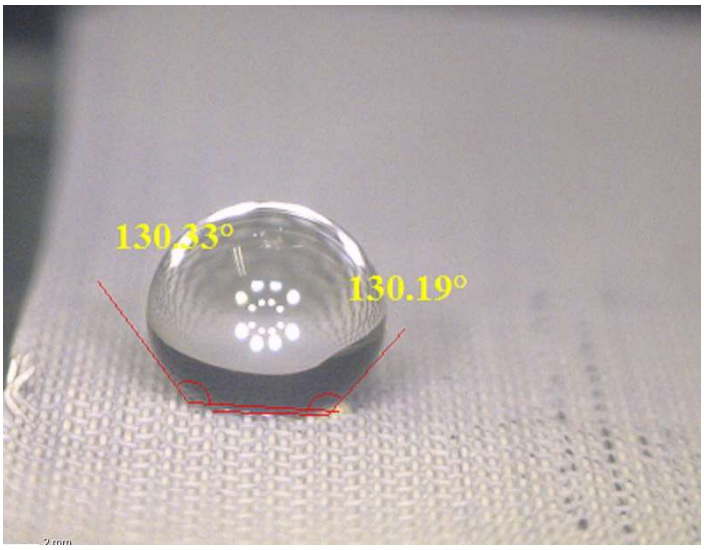


*Note.* Water droplet on 40V electrodeposited stainless steel mesh with static contact angle measurement

Since, from all the above observation it is clear that 20V 10 min shows the best contact angle, we tried to change time for the same voltage to see if we get a better result.

**Figure 4.10**

*Static Contact Angle for Coated Mesh with 20V Electrodeposited Voltage and 5 Minutes Time Duration.*

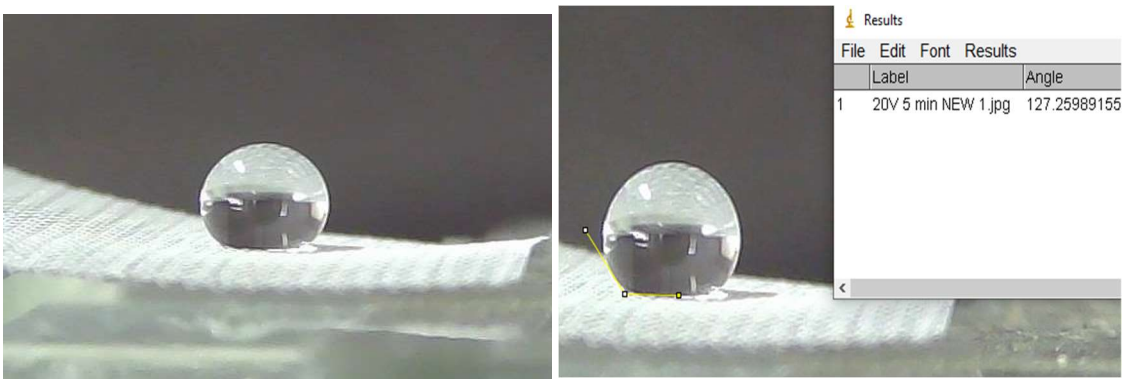


*Note.* Water droplet on 20V 5min electrodeposited stainless steel mesh with static contact angle measurement.

The above figure 4.10 shows the static contact angle for the coated mesh with 20V electrodeposited voltage and 5 minutes time duration. Contact angle was measured to be 127.2° which is very less than the contact angle we measured with 20V and 10 minutes time duration.

Similarly when we measured the contact angle for same voltage but with more time duration i.e 20V and 15 minutes, the static contact angle was measured to be 138.8° as shown in figure 4.11.

**Figure 4.11**

*Static Contact Angle for Coated Mesh with 20V Electrodeposited Voltage and 15 Minutes Time*.

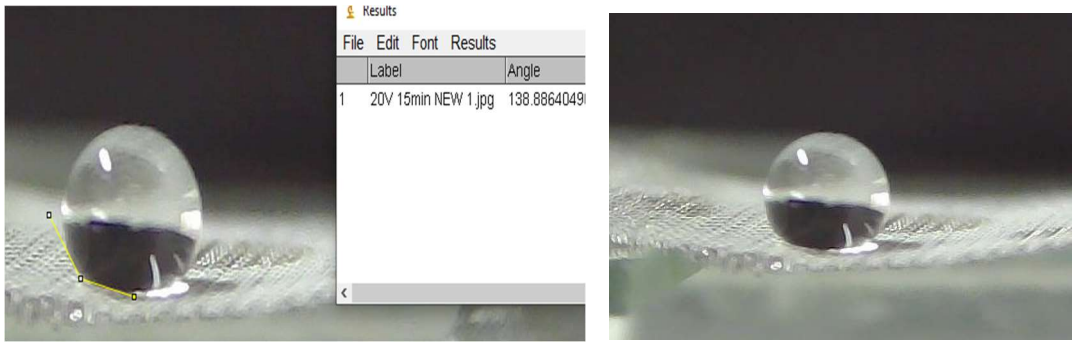


*Note.* Water droplet on 20V 15min electrodeposited stainless steel mesh with static contact angle measurement.

**Figure 4.12**

*Graph Showing Variation of Contact Angle with Voltage.*

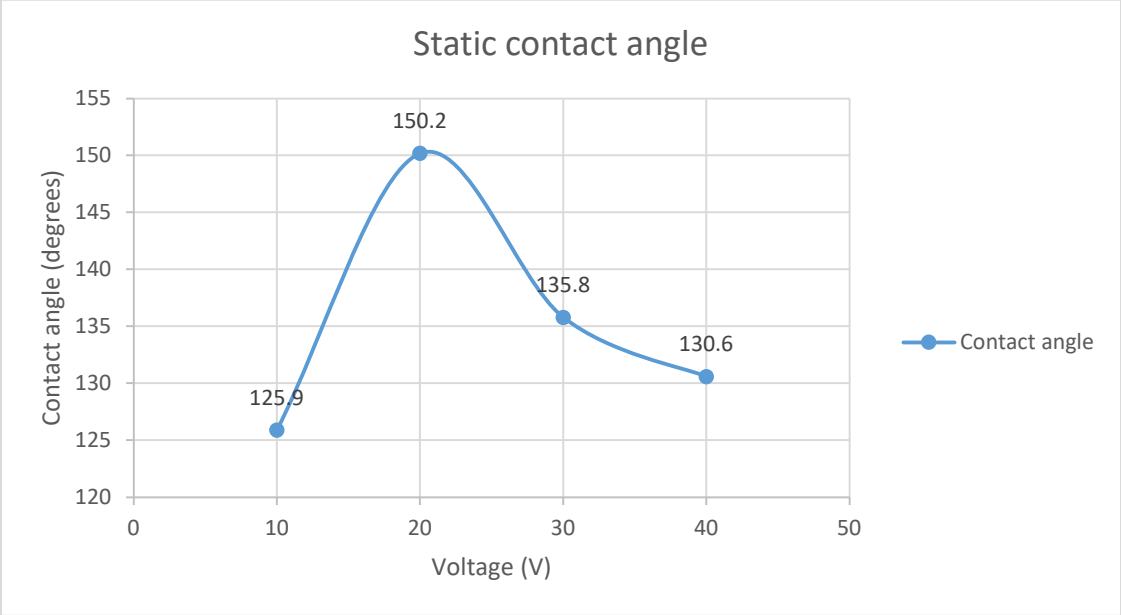


*Note.* Variation of static water contact angle to electrodeposited voltage is shown with graphical representation.

The figure above shows the graphical representation of static contact angle vs electrodeposited voltages. From the graph we can easily observe that the increase in water contact angle is not linear with the increase in voltage. It can be said that it is non-linear. From the FE SEM analysis it is clear we get the most flakes in 20V voltage. As the flakes are formed there are more gaps which is filled by air bubbles and the water droplets can only have contact with the upper part of the flakes which leads to higher contact angle and less sliding angle.

Sliding angle is another parameter which characterizes different surfaces. It also tells us about the deposited nanoparticle. If the contact angle of the surface is higher and water has a spherical shape there is a tendency that the water droplet will roll of faster and the angle will be much lesser.

**Figure 4.13**

*Graph Showing Variation of Sliding Angle with Voltage.*

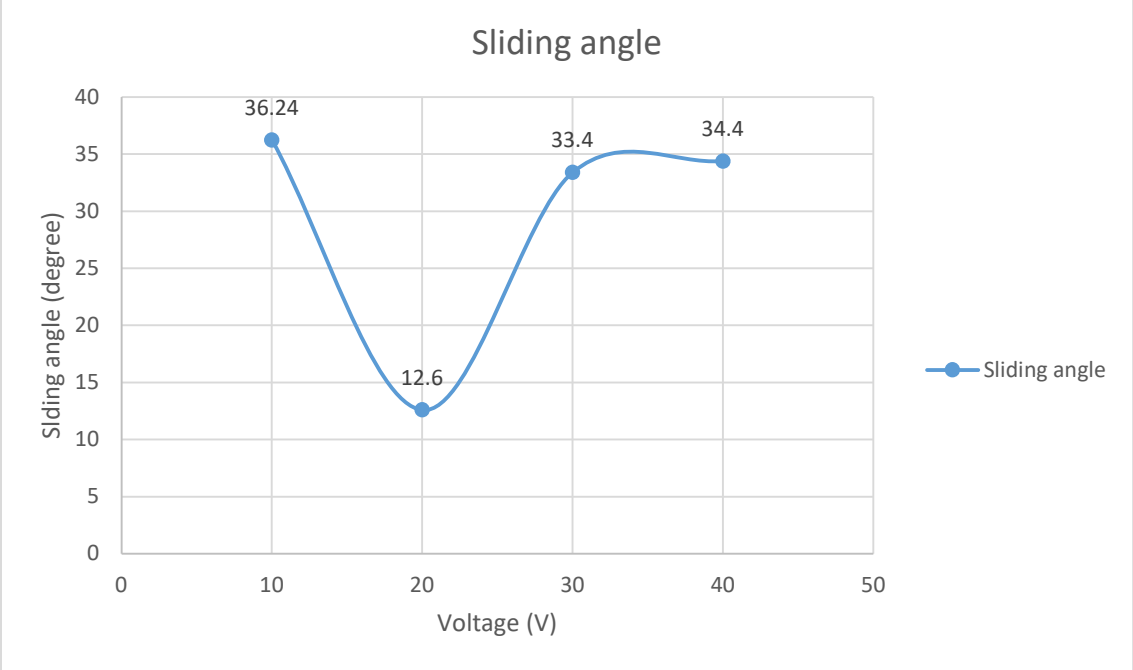


*Note.* Variation of sliding angle to electrodeposited voltage is shown with graphical representation.

The above graph shows the variation of sliding angle vs electrodeposited voltage. Sliding angle is measured by pouring a water droplet on the mesh and kept static for few second. After that we will increase the vertical distance until the droplet slides down. The angle just before the droplet slides is known as sliding angle. Once the clean stainless steel mesh is coated with 10V electrodeposited voltage, we will measure the sliding angle. For this voltage it was measured to be 36.24°. Similarly we did the same procedure for 20V electrodeposited voltage and it was measured to be 12.6°. Again same procedure for 30V electrodeposited voltage, it came to be 33.4° and for 40V electrodeposited voltage the sliding angle measured was 34.4°.

From the graph we can observe that it is non-linear which means with increase of voltage deposition doesn't increase. But it shows the best result for 20V electrodeposited voltage which we already analyzed from our previous SEM results.

**Figure 4.14**

*Graph Showing Stability for 20V Electrodeposited Stainless Steel Mesh.*

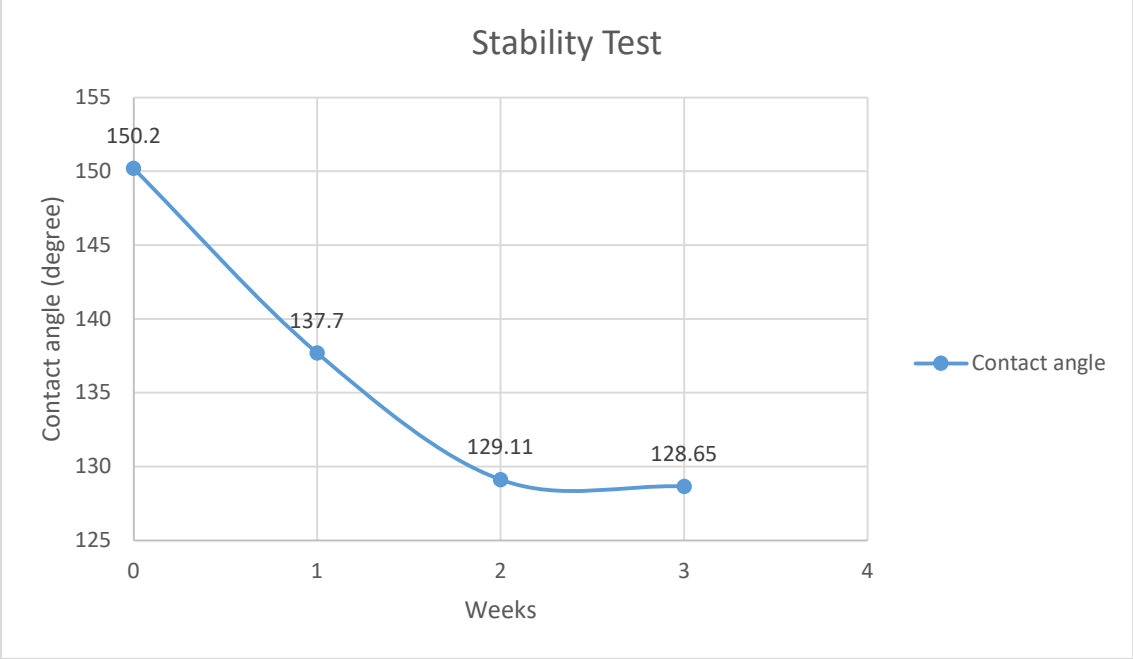


*Note.* Stability test for 20V electrodeposited voltage with contact angle measurement for 3 weeks

The above figure is the graphical representation of stability of coated stainless steel mesh with 20V voltage. There is a linear decrease in contact angle with every week which is clearly visible from the graph. Comparing this to other electrodeposited voltage, for 10V electrodeposited voltage the contact angle also decreases linearly with 125.9° in week 0 (when the sample is newly coated), 119.24° after week 1 (after 7 days), 118.7° after week 2 (after 14 days) to 117.5° after week 3 (after 21 days). Similarly when we talk about 30V electrodeposited voltage it decreases from 135.2° in week 0, 122.7° after 1 week, 121.06° after 2 week to 121.00° after 3 weeks and again for 40V electrodeposited voltage it decreases from 132.2° in week 0, 126.9° after 1 week, 119.21° after 2 week to 118.00° after 3 weeks. From these data it is clear that the nanoparticle deposited in the stainless steel mesh is less stable. Cerium myristate is considered less stable because myristic acid is generally considered to be less table compound.

**Figure 4.15**

*Graph Showing Stability for 20V Electrodeposited Stainless Steel Mesh.*

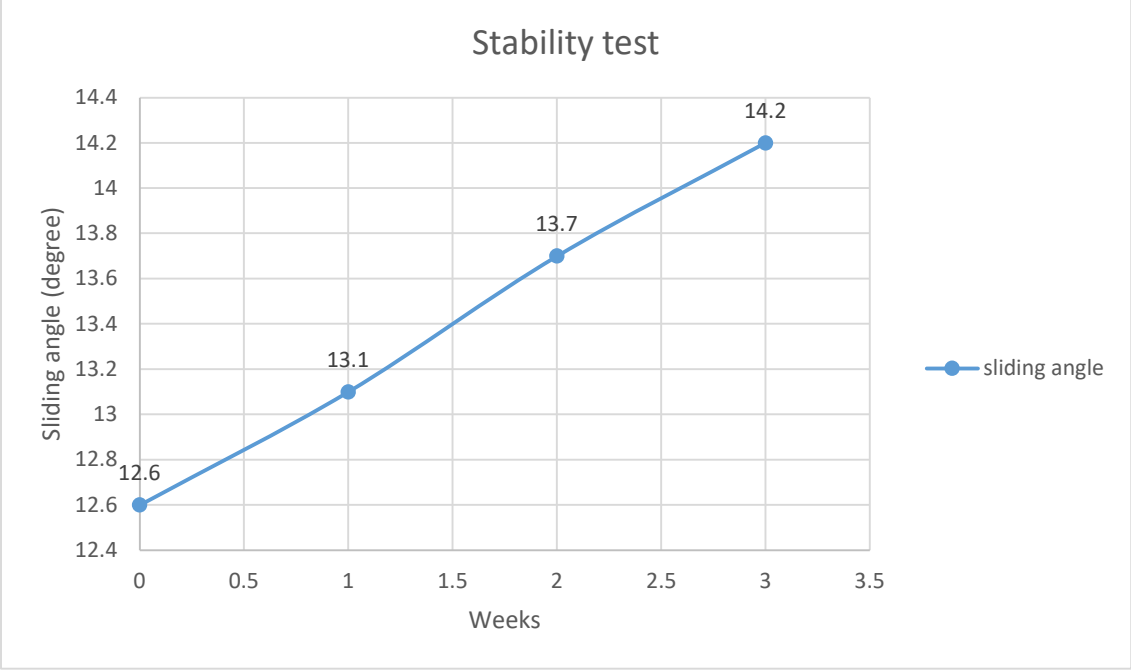


*Note.* Stability test for 20V electrodeposited voltage with sliding angle measurement for 3 weeks

The above figure shows the graphical representation of stability test for 20V electrodeposited mesh. X-axis represents the number of weeks in which week 0 means when the clean stainless steel mesh is just coated with cerium myristate and Y-axis represents the sliding angle for different weeks. Less the sliding angle better the superhydrophobicity, better the roughness and better the wettability. The linear increase in the graph here represents the decrease of stability because of increase in sliding angle. For 10V electrodeposited voltage sliding angle is measured as 36.24° for week 0, 38.58° after 1 week, did not slide after 2 weeks and same after weeks. Similarly for 30V electrodeposited voltage sliding angle was measured to be 33.4° in week 0, 34.0° after 1 week, 34.6° after 2 weeks and 38.4° after 3 weeks. Again for 40V electrodeposited voltage sliding angle was measured to be 34.4° in week 0, 35.3° after 1 week, 36.6° after 2 weeks and 39.5° after 3 weeks. All these data shows the same linear increase in sliding angle after 3 weeks of keeping the coated sample.

### 4.3 Oil Water Separation Analysis

The setup for the oil water separation was made from corning glass tube and a separation design made from 3D printing. As shown in the figure 25, the upper part and lower part of the device was made from cutting corning glass tube of diameter 3cm. The middle part

**Figure 4.16**

*Oil Water Separation Setup*

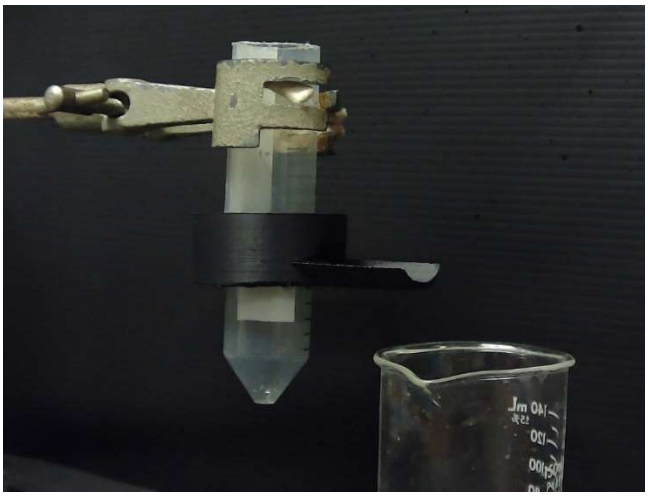

*Note.* Setup for oil water separation.

Here both the tube was fixed is made from 3d printer. The design was made in such a way that it can easily fit the stainless steel mesh of size 3x3 cm. There was a passage made for water to separate and get collected in the beaker and oil goes through.

The experiment of oil water separation was done by collecting 4ml of water (dyed blue with methylene blue) and 1ml of cooking oil in a beaker. The solution of oil and water was stirred continuously for 3-5 minutes. After the solution is made, it is poured through the setup for oil water separation.

**Figure 4.17**

*After Oil Water Separation from the Coated Mesh*

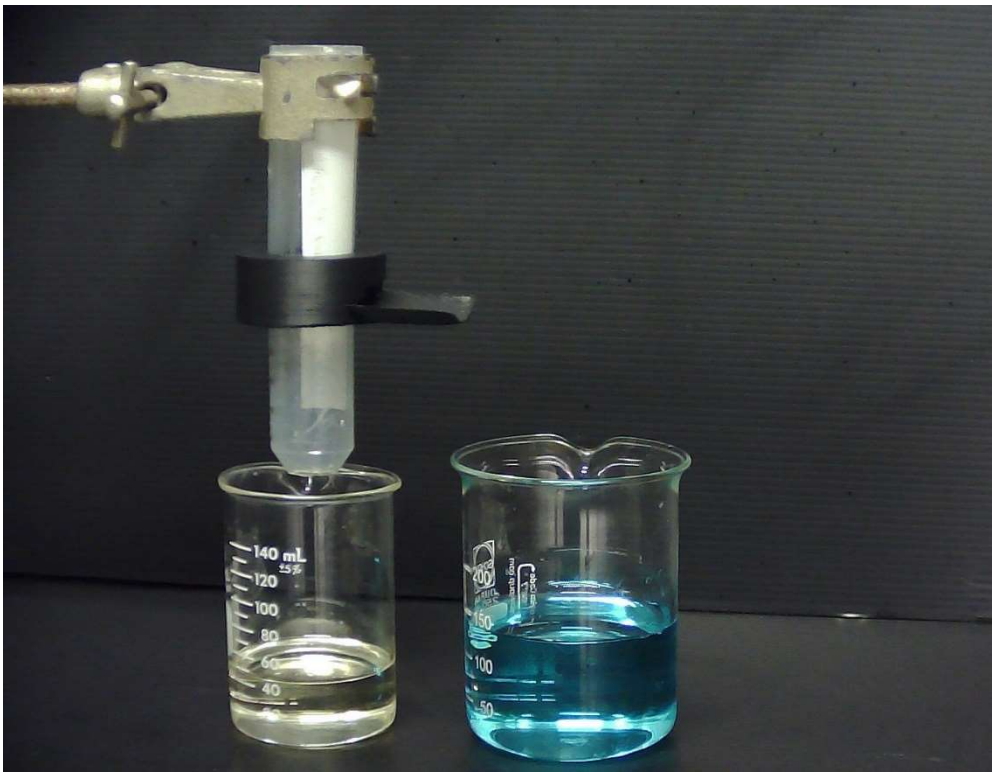


*Note.* Separation of oil water collected in different beaker, blue colored liquid is water

The above figure shows after the separation of oil and water it is collected in different beaker. Water s collected in right had side and oil just passes through the mesh and was collected in another beaker. The efficiency was calculated to be 98.7%, as the coated mesh

achieved superhydrphobicity. Efficiency was calculated by the amount of water collected after separation. As we poured 4ml of water we collected 3.95ml. The same efficiency after we calculated from an uncoated mesh is 95% which means as we pour 4ml of water we collected 3.80ml of water. The coated mesh acts as both superhydrophobic and oleophilic because as we pour the solution the oil passes through the coated mesh faster if we compare that with the uncoated mesh.

The performance of the coated mesh was also analyzed and compared with the uncoated mesh. For that we repeated the same experiment for 10 times both with coated and uncoated sample.

**Figure 4.18**

*Comparison of Efficiency of Coated and Uncoated Mesh.*

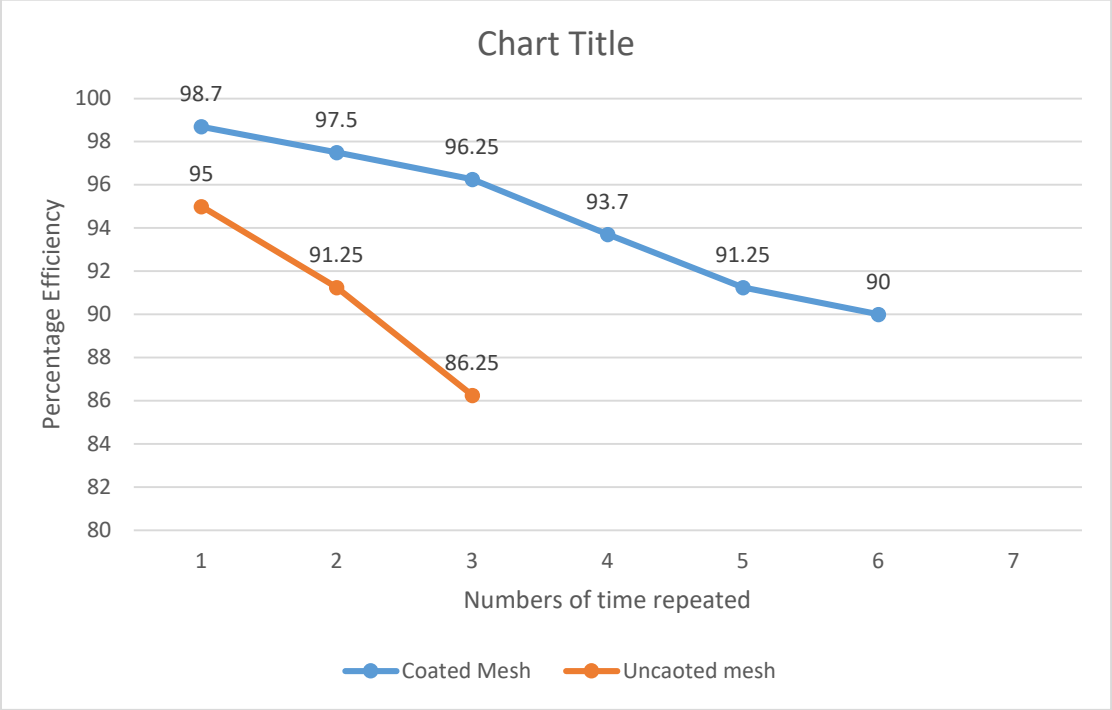


*Note.* The comparison between the percentage efficiency of coated and uncoated is shown.

The efficiency of the coated mesh after we repeated the experiment for several times was 98.7% after 1st time, 97.5% after 2nd time, 96.25% after 3rd time, 93.7% after 4th time,

91.25% after 5$^{th}$ time, 90% after 6$^{th}$ time and after the 7$^{th}$ time the oil mixed with water and collected in beaker.

The same procedure when applied to the uncoated mesh, efficiency was calculated to be 95% after 1$^{st}$ separation, 91.25% after 2$^{nd}$ separation, 86.25% after 3$^{rd}$ separation and after the 4$^{th}$ separation the oil and water started to mix. From this we can say that the coated mesh performance is better than the uncoated mesh. Uncoated mesh performance also decrease rapidly and the experiment can only be repeated for 3 times without oil mixing with water whereas the coated sample can be repeated for 6 times.

# CHAPTER 5
# CONCLUSIONS AND RECOMMENDATIONS

## 5.1 CONCLUSIONS

A superhydrophobic stainless steel mesh coated with cerium myristate was fabricated successfully. The cerium myristate coating was deposited by using a one-step electrodeposition method. Coatings deposited at different applied potentials, varying between 10 V to 40 V, demonstrated variations in terms of their morphology and surface roughness. Coatings obtained at 20 V applied potential demonstrated superhydrophobic nature with water contact angle of 150.1° and sliding angle close to 12°. For other applied voltages that coating was found to be hydrophobic with water contact angles between 130° to 140°. Using the superhydrophobic stainless steel mesh, an oil-water separation filter was fabricated and tested against sunflower oil. Oil was very easily separated by the superhydrophobic mesh and water was separated from the mixture. With the best superhydrophobic mesh an oil separation efficiency of 98.7% was found and the efficiency remained within 90% up to 6 repeated filtration cycles. The results from this study demonstrated an inexpensive and simple oil-water separation superhydrophobic stainless steel mesh that has the potential for future industrial use.

## 5.2 RECOMMENDATIONS

Following recommendations are made for future research:

1) The myristic acid showed low stability in our study. Therefore, alternative of myristic acid for improved filter wetting stability should be investigated.
2) The performance of the filter for different oil-water mixture should be investigated in the future.
3) More detailed electrodeposition conditions should be explored for the controlled and reproducible growth of superhydrophobic coatings on stainless steel mesh.

# REFERENCES


Ariga, K., Hill, J. P., & Ji, Q. (2007). Layer-by-layer assembly as a versatile bottom-up nanofabrication technique for exploratory research and realistic application. *Physical Chemistry Chemical Physics*, *9*(19), 2319–2340. https://doi.org/10.1039/b700410a

Cao, L., Hu, H. A., & Gao, D. (2007). Design and fabrication of micro-textures for inducing a superhydrophobic behavior on hydrophilic materials. *Langmuir*, *23*(8), 4310–4314. https://doi.org/10.1021/la063572r

Celia, E., Darmanin, T., Taffin de Givenchy, E., Amigoni, S., & Guittard, F. (2013). Recent advances in designing superhydrophobic surfaces. *Journal of Colloid and Interface Science*, *402*, 1–18. https://doi.org/10.1016/j.jcis.2013.03.041

Chen, C., Weng, D., Mahmood, A., Chen, S., & Wang, J. (2019). Separation Mechanism and Construction of Surfaces with Special Wettability for Oil/Water Separation [Research-article]. *ACS Applied Materials and Interfaces*, *11*(11), 11006–11027. https://doi.org/10.1021/acsami.9b01293

Chu, Z., Feng, Y., & Seeger, S. (2015). Oil/water separation with selective superantiwetting/superwetting surface materials. *Angewandte Chemie - International Edition*, *54*(8), 2328–2338. https://doi.org/10.1002/anie.201405785

*Disadvantages of Sol Gel Process - Thin Film - Texas Powerful Smart*. (n.d.). Retrieved August 21, 2020, from https://www.texaspowerfulsmart.com/thin-film/disadvantages-of-solgel-process.html

Duta, L., Popescu, A. C., Zgura, I., Preda, N., & Mihailescu, I. N. (2015). Wettability of Nanostructured Surfaces. *Wetting and Wettability*. https://doi.org/10.5772/60808

Gao, S., Dong, X., Huang, J., Li, S., Li, Y., Chen, Z., & Lai, Y. (2018). Rational construction of highly transparent superhydrophobic coatings based on a non-particle, fluorine-free and water-rich system for versatile oil-water separation. *Chemical Engineering Journal*, *333*(July 2017), 621–629. https://doi.org/10.1016/j.cej.2017.10.006

Gupta, R. K., Dunderdale, G. J., England, M. W., & Hozumi, A. (2017). Oil/water separation techniques: A review of recent progresses and future directions. In

*Journal of Materials Chemistry A* (Vol. 5, Issue 31, pp. 16025–16058). Royal Society of Chemistry. https://doi.org/10.1039/c7ta02070h

Jeevahan, J., Chandrasekaran, M., Britto Joseph, G., Durairaj, R. B., & Mageshwaran, G. (2018). Superhydrophobic surfaces: a review on fundamentals, applications, and challenges. *Journal of Coatings Technology and Research*, *15*(2), 231–250. https://doi.org/10.1007/s11998-017-0011-x

Karunakaran, R. G., Lu, C. H., Zhang, Z., & Yang, S. (2011). Highly transparent superhydrophobic surfaces from the coassembly of nanoparticles (≤ 100 nm). *Langmuir*, *27*(8), 4594–4602. https://doi.org/10.1021/la104067c

Li, B., Liu, X., Zhang, X., & Chai, W. (2015). Stainless steel mesh coated with silica for oil-water separation. *European Polymer Journal*, *73*, 374–379. https://doi.org/10.1016/j.eurpolymj.2015.10.031

Li, J. J., Zhou, Y. N., & Luo, Z. H. (2018). Polymeric materials with switchable superwettability for controllable oil/water separation: A comprehensive review. *Progress in Polymer Science*, *87*, 1–33. https://doi.org/10.1016/j.progpolymsci.2018.06.009

Li, X. M., Reinhoudt, D., & Crego-Calama, M. (2007). What do we need for a superhydrophobic surface? A review on the recent progress in the preparation of superhydrophobic surfaces. *Chemical Society Reviews*, *36*(8), 1350–1368. https://doi.org/10.1039/b602486f

Ma, M., Hill, R. M., & Rutledge, G. C. (2008). A review of recent results on superhydrophobic materials based on micro- and nanofibers. In *Journal of Adhesion Science and Technology* (Vol. 22, Issue 15, pp. 1799–1817). Taylor & Francis Group . https://doi.org/10.1163/156856108X319980

Ma, W., Zhao, J., Oderinde, O., Han, J., Liu, Z., Gao, B., Xiong, R., Zhang, Q., Jiang, S., & Huang, C. (2018). Durable superhydrophobic and superoleophilic electrospun nanofibrous membrane for oil-water emulsion separation. *Journal of Colloid and Interface Science*, *532*, 12–23. https://doi.org/10.1016/j.jcis.2018.06.067

Nakajima, A., Hashimoto, K., & Watanabe, T. (2001). Recent studies on super-hydrophobic films. *Monatshefte Fur Chemie*, *132*(1), 31–41. https://doi.org/10.1007/s007060170142

Radjenovic, J., & Sedlak, D. L. (2015). Challenges and Opportunities for Electrochemical Processes as Next-Generation Technologies for the Treatment of Contaminated Water. *Environmental Science and Technology*, *49*(19), 11292–11302. https://doi.org/10.1021/acs.est.5b02414

Rao, P. A., & Engineering, C. (n.d.). *Fabrication of Titanium Dioxide Coated Stainless Steel Mesh Filters for Oil / Water Separation by*. *July 2019*.

Shirtcliffe, N. J., McHale, G., & Newton, M. I. (2011). The superhydrophobicity of polymer surfaces: Recent developments. In *Journal of Polymer Science, Part B: Polymer Physics* (Vol. 49, Issue 17, pp. 1203–1217). John Wiley & Sons, Ltd. https://doi.org/10.1002/polb.22286

Simpson, J. T., Hunter, S. R., & Aytug, T. (2015). Superhydrophobic materials and coatings: A review. In *Reports on Progress in Physics* (Vol. 78, Issue 8, p. 086501). Institute of Physics Publishing. https://doi.org/10.1088/0034-4885/78/8/086501

Wang, L., Yang, S., Wang, J., Wang, C., & Chen, L. (2011). Fabrication of superhydrophobic TPU film for oil-water separation based on electrospinning route. *Materials Letters*, *65*(5), 869–872. https://doi.org/10.1016/j.matlet.2010.12.024

Xiong, Z., Lin, H., Zhong, Y., Qin, Y., Li, T., & Liu, F. (2017). Robust superhydrophilic polylactide (PLA) membranes with a TiO2 nano-particle inlaid surface for oil/water separation. *Journal of Materials Chemistry A*, *5*(14), 6538–6545. https://doi.org/10.1039/c6ta11156d

Zhu, Y., Wang, D., Jiang, L., & Jin, J. (2014). Recent progress in developing advanced membranes for emulsified oil/water separation. *NPG Asia Materials*, *6*(5). https://doi.org/10.1038/am.2014.23